SACLANTCEN REPORT
serial no: SR-266

SACLANT UNDERSEA RESEARCH CENTRE REPORT

MODELING NON-RAYLEIGH REVERBERATION

D.A. Abraham

May 1997

Report no. changed (Mar 2006): SR-266-UU

SACLANT Undersea Research Centre
Viale San Bartolomeo 400
19138 San Bartolomeo (SP), Italy

tel: +39-187-540.111
fax: +39-187-524.600

e-mail: library@saclantc.nato.int

NORTH ATLANTIC TREATY ORGANIZATION

SACLANTCEN SR-266

Modeling non-Rayleigh reverberation

D. A. Abraham

The content of this document pertains to work performed under Project 041-3 of the SACLANTCEN Programme of Work. The document has been approved for release by The Director, SACLANTCEN.

Jan L. Spoelstra
Director

intentionally blank page

Modeling non-Rayleigh reverberation

D. A. Abraham

Executive Summary: Non-Rayleigh reverberation adversely affects the detection performance of submarine and mine hunting sonar systems by increasing the probability of false alarm or decreasing the probability of detection. Prediction of sonar performance in non-Rayleigh reverberation and the design of appropriate target detection algorithms requires accurate statistical modeling of the observed reverberation.

This report presents several standard statistical models for non-Rayleigh reverberation along with methods for estimating their parameters and choosing the model with the best fit. Of the models considered, the Rayleigh mixture model was seen to provide the most flexibility in representing different types of non-Rayleigh reverberation. Real data were used to demonstrate this analysis process, including the examination of theoretical receiver operating characteristic (ROC) curves based on non-Rayleigh reverberation. Matlab subroutines created for parameter estimation, distribution function evaluation, and random number generation are included in an annex.

intentionally blank page

Modeling non-Rayleigh reverberation

D. A. Abraham

Abstract: Researchers over the past three decades have experimentally examined non-Rayleigh reverberation, fitted it to standard distributions such as log-normal and Weibull, developed theoretical models to explain the variation from Rayleigh, and considered new families of distributions appropriate for modeling non-Rayleigh reverberation such as the K and Rayleigh mixture.

This report draws together several of the common statistical models for non-Rayleigh reverberation. Parameter estimates for the Edgeworth expansion, log-normal, Weibull, K, and Rayleigh mixture distributions are presented and evaluated through simulation. Their ability to represent reverberation is examined using the Kolmogorov-Smirnov statistic where it was seen that the Rayleigh mixture provided the most flexibility in representing different types of non-Rayleigh reverberation. In analyzing real reverberation data, a skewness-kurtosis plane is proposed for the initial evaluation of the non-Rayleigh character providing an indication of the viability of each model. The Kolmogorov-Smirnov statistic, or some other appropriate error measure, may then be used to choose the model with the best fit to the observed reverberation. This method is demonstrated on low-frequency active sonar data where the Rayleigh mixture was seen to provide the best fit. Theoretical receiver operating characteristic (ROC) curves are then generated using the estimated Rayleigh mixture proportions and powers and a non-fluctuating target model. The expected loss in detection performance due to the heavier tails of the non-Rayleigh reverberation was clearly observed.

Keywords: non-Rayleigh ○ reverberation ○ statistics

Contents

1 Introduction

Reverberation in active sonar and radar systems is the result of scattering from inhomogeneities in the transmission medium and irregularities in the medium boundaries; for example, reflections from air bubbles near the ocean surface or from the sea floor boundary are observed in sonar and reflections from the sea surface are observed in radar. Reverberation hinders the detection and localization of submarines in active sonar because the reflections inherently are similar to the transmitted signal. Thus, hypothesis testing is used to formulate detectors that help distinguish between a submarine target and reverberation based on a difference in the statistical distribution of their received echoes. The statistics of sea reverberation and radar sea clutter have been subject to substantial theoretical and experimental investigation as evidenced by the extensive, though not exhaustive, list of references in this report. The primary result of these studies has been that the amplitude of the matched filter output due to reverberation is often not Rayleigh distributed. This clearly occurs when the effective number of scatterers insonified by the transmit and receive beampatterns is not large enough for the central limit theorem to hold, resulting in non-Gaussian quadrature and in-phase components of the matched filter output. Alternative distributions have been proposed or derived, including an Edgeworth expansion [8, 1], log-normal [2, 6, 5, 9], Weibull [6, 5], K [22, 23, 24, 14, 15, 13], and mixture or multi-modal Rayleigh [21, 11] distributions. Others have developed their own models including one based on a Markov driven change between two different types of sea-floor patches [3] and a multiplicative model involving chi-squared random variables [7].

The utility of finding an analytical model that adequately represents the distribution of reverberation predominantly lies in the ability to estimate detection and false alarm performance. However, with such knowledge it may also be possible to design better detectors and normalizers or perhaps even to assist in bottom classification. Thus, the researcher is faced with the problem of choosing one of the many possible models for non-Rayleigh reverberation. The first step in this process is the estimation of the parameters characterizing each of the distributions. Then, the distribution that best fits the data must be selected. The intent of this report is to provide the information required to estimate the parameters of some of the more common non-Rayleigh reverberation models and the means to select the one best fitting the data.

2

Parameter estimation for common models

There exist many methods for estimating the parameters of a distribution from observed data [36]. The distribution functions that arise from utilizing parameters estimated from observed data are known as frequency curves in statistics [33]. The primary techniques that have been applied in the formation of frequency curves are the method of moments where the parameters are chosen to equate the first few moments of the model and the data, and the maximum likelihood technique where the parameters are chosen to maximize the likelihood function given the observed data. Other methods exist (see [33]) that may provide better performance depending on how the resulting frequency curves are used.

The maximum likelihood technique, subject to certain regularity conditions, is strongly justified by the consistency and asymptotic efficiency of its estimates [36]. Consistency implies that as the amount of data used to estimate the parameters increases, the estimates converge in probability to the true values. Asymptotic efficiency implies that as more data is used, no other estimator is more efficient (i.e., smaller mean squared error). Unfortunately, it is usually difficult to obtain simple forms for the maximum likelihood estimates and one often is forced to use iterative methods such as the expectation-maximization algorithm [30].

A rather simple and older alternative to maximum likelihood estimation is the method of moments. This technique simply solves the system of equations resulting from equating p moments of a p-parameter model with the equivalent sample moments from the observed data. As the sample moments are consistent estimators for the true moments, the parameter estimates will, in many cases, be consistent as well [37]. The primary disadvantage of the method of moments estimators lies in their inefficiency.

In the following sections the maximum likelihood estimators (MLEs), method of moments estimators (MMEs), or both are presented for the parameters of the Rayleigh, Edgeworth expansion, log-normal, Weibull, K, and Rayleigh mixture distributions along with probability distribution functions (PDFs) and cumulative distribution functions (CDFs). In all cases it is assumed that the matched filter amplitude data used to estimate the parameters $(X_1, X_2, \ldots, X_n)$ are independent and identically distributed with PDF $f_X(x)$ and CDF $F_X(x)$ for $x \geq 0$.

If it is desired to evaluate matched filter magnitude squared data (i.e., $Y_i = X_i^2$), the PDF is

$$f_Y(y) = \frac{1}{2\sqrt{y}} f_X(\sqrt{y}) \tag{1}$$

and the CDF is simply

$$F_Y(y) = F_X(\sqrt{y}) \tag{2}$$

for $y \geq 0$.

Note that the false alarm probability is generally taken to be the probability of the matched-filter magnitude data exceeding a threshold (h) when no signal is present. This is obtained from the CDF according to

$$\begin{aligned} P_{fa}(h) &= \Pr\{X \geq h \,|\text{no signal present}\} \\ &= 1 - F_X(h). \end{aligned} \tag{3}$$

2.1 Rayleigh

The Rayleigh distribution arises in the matched filter magnitude when the quadrature and in-phase components are zero-mean, independent Gaussian random variables with equal variance, a situation occurring if there are enough reflections arriving at any given time for the central limit theorem to hold. The Rayleigh PDF is

$$f_X(x) = \frac{2x}{\lambda} e^{-\frac{x^2}{\lambda}} \tag{4}$$

and the CDF is

$$F_X(x) = 1 - e^{-\frac{x^2}{\lambda}} \tag{5}$$

both for $x \geq 0$ where $\lambda = \mathrm{E}[X^2]$ is the power.

Both the MLE and MME for λ are

$$\hat{\lambda} = \frac{1}{n} \sum_{i=1}^{n} X_i^2 \tag{6}$$

where the $\hat{}$ notation represents an estimator of the parameter it is over. There is a substantial body of literature dedicated to the estimation of the power of a Rayleigh random variable when the data are corrupted by the target and other target-like interferences. These papers usually appear in the context of constant false alarm rate (CFAR) processors for radar or sonar. Gandhi and Kassam [25] present a good description of the current processors with references.

2.2 Edgeworth expansion

The Edgeworth expansion is a series expansion of a PDF with a zero mean normal distribution as the kernel. This expansion is useful in approximating the PDF of random variables with skewness and kurtosis values close to that of the normal distribution. Ol'shevskii [8] utilized an Edgeworth expansion to represent the reverberation process prior to basebanding (so the signal is real and not complex), which under a Rayleigh assumption would be zero-mean Gaussian distributed. Thus, Ol'shevskii sets the skewness to zero (which results from a symmetric assumption for the distribution) and related the kurtosis to the parameters of a Poisson field of scatterers. Assuming that the in-phase and quadrature components of the matched filter output are independent and identically distributed according to such a PDF, the PDF of the matched filter magnitude becomes [1]

$$f_X(x) = \frac{2xe^{-\frac{x}{\lambda}}}{\lambda}\left\{1 + \frac{\gamma}{4!}\left[\frac{3x^4}{\lambda^2} - \frac{12x^2}{\lambda} + 6\right] + \left(\frac{\gamma}{4!}\right)^2\left[\frac{3x^8}{8\lambda^4} - \frac{6x^6}{\lambda^3} + \frac{27x^4}{\lambda^2} - \frac{36x^2}{\lambda} + 9\right]\right\} \quad (7)$$

for $x \geq 0$ where $\frac{\lambda}{2}$ is the variance and γ is the kurtosis of the zero-mean in-phase and quadrature components. It can be seen from eq. (7) that if γ is set to zero, a Rayleigh distribution with power $\lambda = \mathrm{E}\left[X^2\right]$ is obtained. Some tedious analysis results in the CDF

$$F_X(x) = 1 - e^{-z} - \frac{\gamma z e^{-z}}{64}\left[\frac{\gamma z^3}{24} - \frac{\gamma z^2}{2} + \frac{(3\gamma + 16)\,z}{2} - (\gamma + 16)\right] \quad (8)$$

where $z = \frac{x^2}{\lambda}$ for $x \geq 0$.

The premise of the Edgeworth expansion is to approximate the PDF of the observed data by matching the actual and sample moments. If enough moments are used, an accurate approximation may be obtained. Unfortunately, estimates of higher order moments usually have detrimentally high variance. The MME for the power is that found in eq. (6). The fourth moment of the matched filter magnitude provides the required relationship to the kurtosis of the in-phase and quadrature components,

$$\mathrm{E}\left[X^4\right] = \frac{\lambda^2}{2}(\gamma + 4), \quad (9)$$

resulting in

$$\hat{\gamma} = 2\frac{\frac{1}{n}\sum_{i=1}^{n} X_i^4}{\left\{\frac{1}{n}\sum_{i=1}^{n} X_i^2\right\}^2} - 4. \quad (10)$$

A negative kurtosis corresponds to lighter tails in the PDF than the normal distribution. As this is unlikely to be observed, it may be prudent to take the positive part of $\hat{\gamma}$ (i.e., use zero if $\hat{\gamma} < 0$).

2.3 Log-normal

The log-normal PDF is

$$f_X(x) = \frac{\alpha}{\sqrt{2\pi}x} e^{-\frac{(\beta+\alpha\log x)^2}{2}} \tag{11}$$

and takes its name from the fact that a logarithmic transformation

$$Z = \log X \tag{12}$$

results in a normal random variable with mean $\theta = -\frac{\beta}{\alpha}$ and variance $\gamma^2 = \frac{1}{\alpha^2}$. Thus, the CDF of X is

$$\begin{aligned} F_X(x) &= \Pr\{X \le x\} \\ &= \Pr\{Z \le \log x\} \\ &= \Phi(\beta + \alpha \log x) \end{aligned} \tag{13}$$

where

$$\Phi(z) = \int_{-\infty}^{z} \frac{1}{\sqrt{2\pi}} e^{-\frac{z^2}{2}} \tag{14}$$

is the CDF of a standard normal random variable.

Due to the invariance of maximum likelihood estimation under a logarithmic transformation, the MLEs for α and β may be determined from the MLEs for θ and γ^2,

$$\hat{\alpha}_{\text{MLE}} = \frac{1}{\hat{\gamma}} \tag{15}$$

and

$$\hat{\beta}_{\text{MLE}} = -\frac{\hat{\theta}}{\hat{\gamma}} \tag{16}$$

where

$$\hat{\theta} = \frac{1}{n}\sum_{i=1}^{n} \log X_i \tag{17}$$

and

$$\hat{\gamma}^2 = \frac{1}{n}\sum_{i=1}^{n} \left(\log X_i - \hat{\theta}\right)^2. \tag{18}$$

The mean and power of the matched filter magnitude are

$$\mu = \mathrm{E}[X] = e^{\frac{1}{2\alpha^2} - \frac{\beta}{\alpha}} \tag{19}$$

and

$$\lambda = \mathrm{E}\left[X^2\right] = \mu^2 \mathrm{e}^{\frac{1}{\alpha^2}}. \tag{20}$$

The MMEs for α and β are obtained by inverting these equations and substituting in the first two sample moments,

$$\hat{\alpha}_{\mathrm{MME}} = \left[\log\left(\frac{\hat{\lambda}}{\hat{\mu}^2}\right)\right]^{\frac{1}{2}} \tag{21}$$

and

$$\hat{\beta}_{\mathrm{MME}} = \frac{1}{2\hat{\alpha}_{\mathrm{MME}}} - \hat{\alpha}_{\mathrm{MME}} \log \hat{\mu} \tag{22}$$

where $\hat{\lambda}$ is as in eq. (6) and

$$\hat{\mu} = \frac{1}{n}\sum_{i=1}^{n} X_i. \tag{23}$$

It is interesting to note that if X is log-normally distributed, then so is $Y = X^2$; that is, the log-normal distribution is self-repeating under a power-law transformation. This implies that approximating either the matched filter magnitude or magnitude squared output by a log-normal random variable results in the same fit. Johnson, Kotz, and Balakrishnan [34] provide more detail on the properties, background, and usage of the log-normal distribution.

2.4 Weibull

The Weibull PDF has the form

$$f_X(x) = \alpha\beta x^{\beta-1} \mathrm{e}^{-\alpha x^\beta} \tag{24}$$

for $x \geq 0$ where it is seen that the Rayleigh ($\beta = 2$) and exponential ($\beta = 1$) distributions may be obtained by the appropriate choice of β. The CDF is easily seen to be

$$F_X(x) = 1 - \mathrm{e}^{-\alpha x^\beta}. \tag{25}$$

Johnson, Kotz, and Balakrishnan [34] indicate that the easiest way to obtain the MLEs for α and β is to utilize a logarithmic transformation ($Z = \log X$) which results in an extreme value distribution (see [35]) with PDF

$$f_Z(z) = \frac{1}{\psi} \exp\left\{-\frac{(z-\zeta)}{\psi} - \mathrm{e}^{-\frac{(z-\zeta)}{\psi}}\right\} \tag{26}$$

where

$$\psi = -\frac{1}{\beta} \tag{27}$$

and

$$\zeta = \frac{-\log \alpha}{\beta}. \tag{28}$$

Johnson, Kotz, and Balakrishnan [35] describe an iterative technique for obtaining the MLE for ψ. First, initialize $\hat{\psi}$ by equating the theoretical and sample variances,

$$\hat{\psi} = -\frac{\sqrt{6}}{\pi}\hat{\gamma} \tag{29}$$

where $\hat{\gamma}$ is, as in eq. (18), the sample standard deviation of the $Z_i = \log X_i$. Then perform the following iteration until convergence,

$$\begin{aligned} \hat{\psi} &:= \hat{\theta} - \frac{\sum_{i=1}^{n} Z_i \mathrm{e}^{-\frac{Z_i}{\hat{\psi}}}}{\sum_{i=1}^{n} \mathrm{e}^{-\frac{Z_i}{\hat{\psi}}}} \\ &= \hat{\theta} - \frac{\sum_{i=1}^{n} X_i^{-\frac{1}{\hat{\psi}}} \log X_i}{\sum_{i=1}^{n} X_i^{-\frac{1}{\hat{\psi}}}} \end{aligned} \tag{30}$$

where $\hat{\theta}$ is, as in eq. (17), the sample mean of the Z_i. The MLE for ζ then follows as

$$\begin{aligned} \hat{\zeta} &= -\hat{\psi} \log \left\{ \frac{1}{n} \sum_{i=1}^{n} \mathrm{e}^{-\frac{Z_i}{\hat{\psi}}} \right\} \\ &= -\hat{\psi} \log \left\{ \frac{1}{n} \sum_{i=1}^{n} X_i^{-\frac{1}{\hat{\psi}}} \right\}. \end{aligned} \tag{31}$$

The MLEs for α and β are formed by inverting eqs. (27) and (28) and substituting the MLEs of ψ and ζ,

$$\hat{\alpha}_{\mathrm{MLE}} = \mathrm{e}^{\frac{\hat{\zeta}}{\hat{\psi}}} \tag{32}$$

and

$$\hat{\beta}_{\mathrm{MLE}} = -\frac{1}{\hat{\psi}}. \tag{33}$$

If X is Weibull distributed with the parameterization described by the PDF found in eq. (24), its mean and power are, respectively,

$$\mu = \mathrm{E}[X] = \alpha^{-\frac{1}{\beta}} \Gamma\left(1 + \frac{1}{\beta}\right) \tag{34}$$

and

$$\lambda = \alpha^{-\frac{2}{\beta}} \Gamma\left(1 + \frac{2}{\beta}\right). \tag{35}$$

The MMEs for α and β are found by inverting eqs. (34) and (35) and substituting in the first two sample moments ($\hat{\mu}$ and $\hat{\lambda}$). Unfortunately, functional inversion of the Gamma function $\Gamma(x)$ is not possible in closed form. Thus, the function

$$h(b) = \frac{\{\Gamma(1+b)\}^2}{\Gamma(1+2b)} - \frac{\hat{\mu}^2}{\hat{\lambda}} \tag{36}$$

is formed so that when $h(b^*) = 0$, the value of $\hat{\beta}_{\text{MME}} = \frac{1}{b^*}$ combined with

$$\hat{\alpha}_{\text{MME}} = \left[\frac{\Gamma\left(1 + \frac{1}{\hat{\beta}_{\text{MME}}}\right)}{\hat{\mu}}\right]^{\hat{\beta}_{\text{MME}}} \tag{37}$$

will satisfy eqs. (34) and (35) after substitution of the first two sample moments. The Newton-Raphson iteration may be applied to find the root of $h(b)$,

$$b := b - \frac{h(b)}{h'(b)} \tag{38}$$

where

$$h'(b) = 2\frac{\Gamma(1+b)}{\{\Gamma(1+2b)\}^2}\left[\Gamma'(1+b)\Gamma(1+2b) - \Gamma(1+b)\Gamma'(1+2b)\right] \tag{39}$$

and $\Gamma'(x)$ may be related to the digamma (ψ) function for which a complete description with an algorithm for numerical evaluation is available in [42]. The Newton-Raphson iteration should be initialized somewhere reasonable, for instance with $b = \frac{1}{\beta} = \frac{1}{2}$ which results in a Rayleigh PDF.

2.5 K-distribution

The K-distribution was first used to describe the statistics of sea surface clutter in radar by Jakeman and Pusey [18], generating a substantial body of literature throughout the ensuing years including [22, 23, 24, 26, 20, 16, 14, 15, 13, 27, 19, 17]. Jakeman and Tough [26] indicate that the K-distribution is the limiting distribution obtained when the number of scatterers is negative binomial distributed. The limit is taken as the average number of scatterers goes to infinity. Were the number of scatterers Poisson distributed, the limiting distribution would be Rayleigh. Ward [22] described the K-distribution as the result of the product of two independent random variables,

$$X = ZY \tag{40}$$

where Z is slowly fluctuating in time and chi-distributed (i.e., the square root of a chi-squared or, more generally, a gamma distributed random variable)

$$f_Z(z) = \frac{2z^{2\nu-1}e^{-z^2}}{\Gamma(\nu)} \tag{41}$$

and Y is rapidly fluctuating and Rayleigh distributed with power α

$$f_Y(y) = \frac{2ye^{-\frac{y^2}{\alpha}}}{\alpha}. \tag{42}$$

The strength of this description is its flexibility in describing the correlation observed from ping to ping in radar sea clutter data with the slowly fluctuating chi-distributed component which modulates the typical Rayleigh return from multiple scatterers [24]. Additionally, the K-distribution allows representation of a target within the reverberation [15, 24].

The K-distribution PDF is found by noting that the distribution of X given Z is simply Rayleigh with power αZ^2 and then integrating over Z, resulting in

$$f_X(x) = \frac{4}{\sqrt{\alpha}\Gamma(\nu)}\left(\frac{x}{\sqrt{\alpha}}\right)^{\nu} K_{\nu-1}\left(\frac{2x}{\sqrt{\alpha}}\right) \tag{43}$$

for $x \geq 0$ where $K_{\nu-1}(x)$ is the $\nu - 1$ order modified Bessel function. The CDF follows immediately

$$F_X(x) = 1 - \frac{1}{\Gamma(\nu)2^{\nu-1}}\left(\frac{2x}{\sqrt{\alpha}}\right)^{\nu} K_{\nu}\left(\frac{2x}{\sqrt{\alpha}}\right) \tag{44}$$

where the following relationship [42] has been exploited

$$\int_0^x t^{\nu} K_{\nu-1}(t)\,dt = 2^{\nu-1}\Gamma(\nu) - x^{\nu}K_{\nu}(x) \tag{45}$$

for $\nu > 0$. It is fairly straightforward to show that a Rayleigh distribution with power α is obtained from the K-distribution in the limit as $\nu \to \infty$ when the scale $\frac{1}{\sqrt{\nu}}$ is applied to X.

Considering the PDF of eq. (43), estimation of α and ν for the K-distribution certainly seems to be a formidable problem. Ward [23] provided an empirical formula for ν based on the grazing angle and cross-range resolution of a vertically polarized radar. Raghavan [20] proposed an estimator based on approximating the K-distribution by a gamma distribution. The estimators resulted in a form depending on the arithmetic and geometric sample means that perform well when the K-distribution is distinctly non-Rayleigh. Joughin *et al.* [27] present an analysis of the MLEs for the parameters obtained through a numerical maximization of the likelihood function. They compared the MLE to Raghavan's method [20] and

method of moment estimators based on either the first and second or second and fourth moments. Simulation analysis showed that the MLE performed best when ν is small with Raghavan's method being nearly equivalent and that when ν is large the method of moments estimator using the first two moments performs best with the MLE being nearly equivalent.

Based on the results of Joughin *et al.* [27] the method of moments estimator using the first two moments is recommended, providing an acceptable trade-off between performance and difficulty of implementation. Due to the independence of Y and Z, the moments of X are easily shown to be

$$\begin{aligned} \mathrm{E}\left[X^i\right] &= \mathrm{E}\left[Z^i\right]\mathrm{E}\left[Y^i\right] \\ &= \alpha^{\frac{i}{2}}\Gamma\left(1+\frac{i}{2}\right)\frac{\Gamma\left(\nu+\frac{i}{2}\right)}{\Gamma(\nu)}. \end{aligned} \tag{46}$$

Matching the second moment results in choosing

$$\hat{\lambda} = \alpha\nu \tag{47}$$

which, when solved for α and substituted into the relationship for the first moment results in

$$\hat{\mu} = \frac{1}{2}\sqrt{\frac{\pi\hat{\lambda}}{\nu}}\frac{\Gamma\left(\nu+\frac{1}{2}\right)}{\Gamma(\nu)}. \tag{48}$$

No closed form solution is obtainable for ν due to the gamma functions. Thus, as with the Weibull MLE, the Newton-Raphson root finding algorithm is applied to the function

$$h(\nu) = \frac{4\nu\Gamma^2(\nu)}{\pi\Gamma^2\left(\nu+\frac{1}{2}\right)} - \frac{\hat{\lambda}}{\hat{\mu}^2} \tag{49}$$

which has derivative

$$h'(\nu) = \frac{4\Gamma^2(\nu)}{\pi\Gamma^2\left(\nu+\frac{1}{2}\right)}\left\{1+2\nu\left[\psi(\nu)-\psi\left(\nu+\frac{1}{2}\right)\right]\right\} \tag{50}$$

where

$$\psi(\nu) = \frac{\Gamma'(\nu)}{\Gamma(\nu)} \tag{51}$$

is the digamma function [42]. Note that for large ν most algorithms evaluating the gamma function will have problems. Application of Stirling's approximation [39] to the gamma function results in

$$\frac{\Gamma(\nu)}{\Gamma\left(\nu+\frac{1}{2}\right)} \approx \frac{1}{\sqrt{\nu}}\left[\frac{\mathrm{e}^{\frac{1}{2}}}{\left(1+\frac{1}{2\nu}\right)^{\nu}}\right]\left[1+\frac{1}{2\nu(12\nu+7)}\right] \tag{52}$$

which should be used for $\nu > 20$. For numerical reasons the Newton-Raphson root finding iteration may have difficulty when ν is small with $h(\nu)$. In these situations the function

$$g(\nu) = \frac{1}{\frac{4\nu\Gamma^2(\nu)}{\pi\Gamma^2\left(\nu+\frac{1}{2}\right)}} - \frac{\hat{\mu}^2}{\hat{\lambda}} \tag{53}$$

and its derivative

$$g'(\nu) = \frac{h'(\nu)}{\left\{\frac{4\nu\Gamma^2(\nu)}{\pi\Gamma^2\left(\nu+\frac{1}{2}\right)}\right\}^2} \tag{54}$$

are better suited.

In both cases, a reasonable initial estimate of ν is obtained from using the approximation of eq. (52) without the third multiplicative term in eq. (49) with $h(\nu) = 0$. Applying a second order approximation to $\log\left(1 + \frac{1}{2\nu}\right)$ then results in the starting point

$$\hat{\nu} = \frac{1}{4}\left[\log\left(\frac{\hat{\lambda}}{\hat{\mu}^2}\right) - \log\left(\frac{4}{\pi}\right)\right]^{-1}. \tag{55}$$

After the Newton-Raphson iteration

$$\hat{\nu} := \hat{\nu} - \frac{h(\hat{\nu})}{h'(\hat{\nu})} \tag{56}$$

has converged, α is estimated according to eq. (47)

$$\hat{\alpha} = \frac{\hat{\lambda}}{\hat{\nu}}. \tag{57}$$

2.6 Rayleigh Mixture

Suppose that a particular sea-bottom were composed of two distinct types of materials; for example, sand with interspersed patches of shells. Crowther [3] attempted to describe this situation with a Markov driven change between two types of reverberation. A mixture of Rayleigh random variables may represent such reverberation well with the added benefit of a much simpler model. If the reverberation were to come from the sand with probability $1 - \epsilon$ and power λ_0 and from the shells with probability ϵ and power λ_1, the PDF would be

$$f_X(x) = (1-\epsilon)\,\frac{2x}{\lambda_0}\,\mathrm{e}^{-\frac{x^2}{\lambda_0}} + \epsilon\,\frac{2x}{\lambda_1}\,\mathrm{e}^{-\frac{x^2}{\lambda_1}} \tag{58}$$

which is known as a Rayleigh mixture where ϵ is the mixture proportion. This, of course, may be generalized to m mixture components, resulting in the PDF

$$f_X(x) = \sum_{i=1}^{m} \epsilon_i \frac{2x}{\lambda_i} \mathrm{e}^{-\frac{x^2}{\lambda_i}} \tag{59}$$

and the CDF

$$F_X(x) = 1 - \sum_{i=1}^{m} \epsilon_i \mathrm{e}^{-\frac{x^2}{\lambda_i}} \tag{60}$$

where

$$\sum_{i=1}^{m} \epsilon_i = 1 \tag{61}$$

is required to ensure a valid CDF.

Trunk [21] considered a two component mixture of zero-mean Gaussian random variables as a possible model for the in-phase and quadrature components of the matched filter output. Though this model is reasonable, it allows the quadrature and in-phase components to come from different parts of the mixture. Stewart *et al.* [11] more appropriately consider Rayleigh mixtures with two or four components. However, starting with a mixture of zero-mean complex Gaussian random variables results in the Rayleigh mixture PDF of eq. (59) and also allows for the inclusion of target models. A non-fluctuating or deterministic target results in a mixture of Rician random variables. A Rayleigh fluctuating target (i.e., Swerling type I or II) results in a mixture of Rayleigh random variables with powers $\lambda_i + \lambda_0$ where λ_0 is the power contributed by the target and the λ_i are, as in eq. (59), the powers of the individual mixture components. The ability to consider various target models in the presence of non-Rayleigh reverberation means that receiver operating characteristic curves (i.e., probability of detection vs. probability of false alarm) may be generated as long as the reverberation is well modelled by a Rayleigh mixture. Fortunately, mixture distributions are known for their flexibility in modeling probability density functions [44, 38].

In modeling reverberation with a Rayleigh mixture, the number of mixture components, their proportions and powers must be chosen. Stewart *et al.* [11] chose these by varying them until there was a good visual match between the estimated PDF and the Rayleigh mixture PDF. Fortunately, a method more suitable to automation exists for estimating the mixture component parameters. Given the number of components, the MLEs for the mixture component proportions and powers may be obtained iteratively through the expectation-maximization (EM) algorithm [30, 40]. The Rayleigh PDF is a member of the exponential class of PDFs [32], for which the EM iteration is straightforward [40]. Given the data $\{X_1, \ldots, X_n\}$ and an initial set

of estimates of the mixture proportions $\{\hat{\epsilon}_1, \ldots, \hat{\epsilon}_m\}$ and powers $\left\{\hat{\lambda}_1, \ldots, \hat{\lambda}_m\right\}$, the intermediate values

$$W_{i,j} = \frac{\hat{\epsilon}_i \, g\left(X_j; \hat{\lambda}_i\right)}{\sum_{k=1}^{m} \hat{\epsilon}_k \, g\left(X_j; \hat{\lambda}_k\right)} \tag{62}$$

are formed for $i = 1, \ldots, m$ and $j = 1, \ldots, n$ where

$$g(x; \lambda) = \frac{2x}{\lambda} \, \mathrm{e}^{-\frac{x^2}{\lambda}} \tag{63}$$

is a single Rayleigh PDF. New values of the mixture proportions are then formed according to

$$\hat{\epsilon}_i := \frac{1}{n} \sum_{j=1}^{n} W_{i,j} \tag{64}$$

and their associated powers as

$$\hat{\lambda}_i := \frac{\sum_{j=1}^{n} X_j^2 W_{i,j}}{\sum_{j=1}^{n} W_{i,j}} \tag{65}$$

until convergence. As the EM algorithm converges to local and not global maxima, it may be appropriate to run the iteration from several initial starting points. A reasonable choice for the mixture proportions is to initialize them to be equally likely,

$$\hat{\epsilon}_i = \frac{1}{m}. \tag{66}$$

Reasonable choices for the power components are either (i) the sample powers formed from m disjoint subsets of the n data samples, or (ii) the sample powers formed from m subsets of the n ordered data samples so that $\hat{\lambda}_i < \hat{\lambda}_{i+1}$. Choice of the model order poses a slightly more difficult problem. It is possible to apply Akaike's information criterion (AIC) [29] or Rissanen's minimum descriptive length (MDL) criterion [41] to choose the model order. As these require evaluation of the MLEs for several model orders, other equally justifiable methods include evaluation of the Kolmogorov-Smirnov statistic [31] or consideration of the mixture component proportions and powers (i.e., if an additional component results in a near zero proportion or a power identical to a component already present, the lower order model is likely adequate). The reader is referred to [40, 30, 44, 43] for further information on the EM algorithm and its properties.

3
Choosing a model

The previous section provides a set of probability distributions that may be used to model reverberation along with the means to estimate their parameters. Choosing a model may require consideration of

- the physical phenomenon creating the reverberation (i.e., if there is a justifiable relationship between the physics and one of the PDF models), and
- how the model is to be used (i.e., if an on-line normalizer is to be implemented the parameter estimation must be rapid and accurate with minimal data, if ROC curves are to be generated a large amount of data will be required for accuracy at small false alarm probabilities).

In this section, the skewness and kurtosis descriptors are evaluated for each of the PDF models to illustrate their generality or narrowness in representing higher-order moments. This type of analysis is the first step in choosing which reverberation models are appropriate for further consideration. Given several competing models for representing the reverberation PDF, the Kolmogorov-Smirnov statistic is evaluated through simulation for choosing the model with the best fit.

3.1 Skewness and kurtosis descriptors

One method of comparing the capability of a PDF family to represent a variety of distributions is to consider a graphical representation of the possible values of skewness and kurtosis that the PDF may represent. Skewness and kurtosis are measures of departure from normality. A high kurtosis represents an excess of values near the mean of the distribution and far from it (i.e., in the tails). Skewness represents non-symmetry in the PDF. Johnson, Kotz, and Balakrishnan [34] present curves relating these descriptors using $\beta_1 = \gamma_3^2$ and $\beta_2 = \gamma_4 + 3$ where

$$\gamma_3 = \frac{\mathrm{E}\left[(x-\mu)^3\right]}{\sigma^3} \tag{67}$$

is the skewness,

$$\gamma_4 = \frac{\mathrm{E}\left[(x-\mu)^4\right]}{\sigma^4} - 3 \tag{68}$$

is the kurtosis, $\mu = \mathrm{E}[X]$ is the mean, and $\sigma^2 = \mathrm{E}\left[(X-\mu)^2\right]$ is the variance.

The Rayleigh distribution is fully represented by a single scale parameter. As the skewness and kurtosis are scale invariant descriptors, the Rayleigh distribution is represented as a single point in the (β_2, β_1) plane, specifically,

$$\beta_1 = \frac{4\pi(\pi-3)^2}{(4-\pi)^3} \tag{69}$$

and

$$\beta_2 = \frac{32-3\pi^2}{(4-\pi)^2}. \tag{70}$$

The Edgeworth expansion (as applied here), Weibull, log-normal, and K-distributions are all two parameter models, one of which is a scale parameter. Thus, they are represented as lines in the (β_2, β_1) plane. A two component Rayleigh mixture is a three parameter model, resulting in a region in the (β_2, β_1) plane. Annex A contains either the skewness and kurtosis values or the information required to obtain them for each of the distributions considered. Figure 1 shows the relationships between β_1 and β_2 for each of the distributions as well as the upper limit on β_1 for all distributions [34],

$$\beta_1 \leq \beta_2 - 1. \tag{71}$$

Estimates of β_1 and β_2 from real data can provide an indication of which PDFs are appropriate to consider. However, matching skewness and kurtosis does not imply that distributions are identical or even a good approximation to one another.

3.2 Kolmogorov-Smirnov statistics

The Kolmogorov-Smirnov (KS) test statistic is [31]

$$T_n = \sqrt{n} \max_{-\infty<x<\infty} |F(x;\theta) - S_n(x)| \tag{72}$$

where $F(x;\theta)$ is the candidate analytical CDF as a function of the parameter vector θ and $S_n(x)$ is the sample CDF formed from n samples of data. Thus, if $F(x;\theta)$ is the

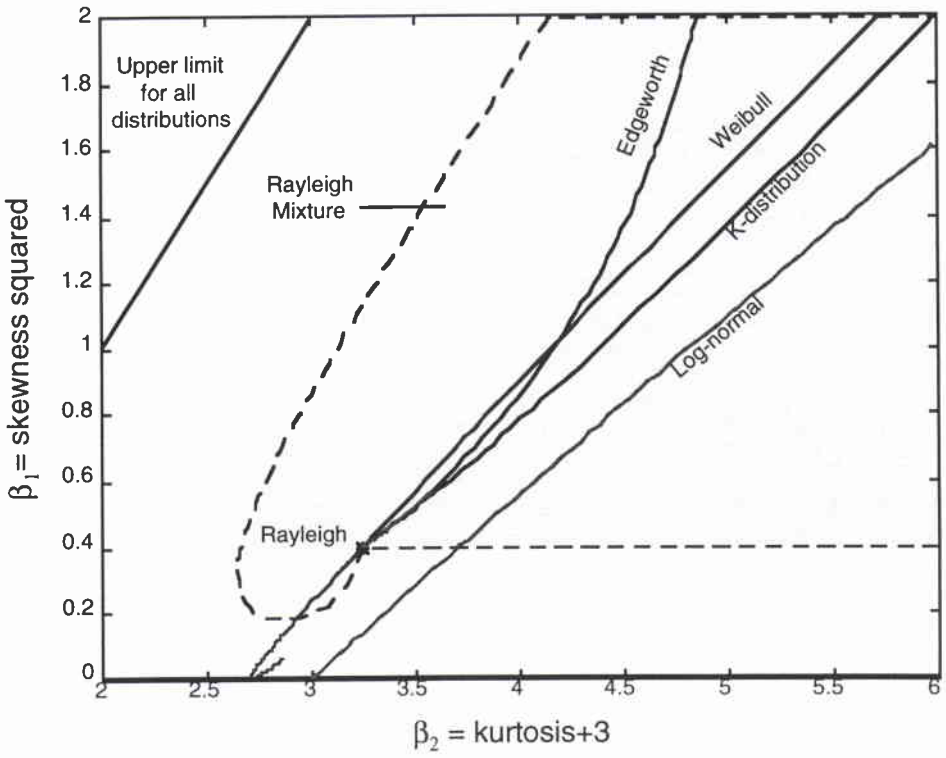

Figure 1 *(β_2, β_1) plane showing upper limit for all distributions, Rayleigh point, Weibull, log-normal, K-distribution, and Edgeworth expansion lines, and region for a two component Rayleigh mixture.*

true distribution or a good model, T_n will be small. Kolmogorov's theorem indicates that as $n \to \infty$, the CDF of T_n goes to the function

$$\begin{aligned} Q(h) &= \lim_{n\to\infty} \Pr\{T_n < h\} \\ &= \sum_{i=-\infty}^{\infty} (-1)^i \, \mathrm{e}^{-2i^2h^2} \end{aligned} \tag{73}$$

if $F(x;\theta)$ is the CDF of the observed data. As stated in Fisz [31], Kolmogorov's theorem does not hold when parameters estimated from the data are used to form the theoretical CDF. Nevertheless, transforming the KS statistic to the (now approximate) p-value (i.e., $p = 1 - Q(T_n)$) should roughly indicate the probability of observing a value greater than T_n given that $F(x;\theta)$ is the true CDF of the data. Additionally, as it is a monotonically decreasing transformation, order is preserved. This implies that an analytical CDF with a smaller KS statistic (i.e., better fit) than some alternative CDF correspondingly has a larger p-value.

The ability to consider approximate p-values is a strong argument for utilizing the KS statistic in choosing a model CDF. However, depending on how the model CDF is to be used, other performance measures may be appropriate. For example, if the CDF model is used to generate ROC curves or to choose thresholds for a detector, then accuracy in the tails of the distribution should be emphasized. This may be accomplished by considering the squared error between the candidate and sample exceedance probability functions (i.e., one minus the CDF which is usually taken as the probability of false alarm) for specific threshold values or the squared error between the estimated and theoretical thresholds (quantiles) for a specific range of probabilities of false alarm. Such performance measures may also be used to estimate the parameters of a distribution using numerical maximization techniques (i.e., minimize the error measure rather than maximizing the likelihood function or matching the moments).

Regardless of which performance measure is used to choose the best fitting model, the fit is made to the sample CDF as estimated from the observed data. Thus, a good fit (as indicated by a low KS statistic, large KS statistic p-value, or other performance measure) does not assure accurate estimation of the underlying CDF, only accurate approximation of the estimated CDF. Enough data to estimate the CDF to the desired accuracy is crucial, particularly when the tails of the distribution are of interest.

3.3 MLE or MME?

Both the maximum likelihood and method of moments estimators have been presented in Section 2 for the Weibull and log-normal distributions. Both have equivalent numerical implementation requirements, so simulation is used to determine

which one is better. The p-value of the KS statistic and the CDF error measure

$$e = \Delta \sum_{i=1}^{M} \left[F(i\Delta;\theta) - F\left(i\Delta;\hat{\theta}\right) \right]^2 \tag{74}$$

are considered where θ is the true parameter vector, $\hat{\theta}$ is either the MLE or MME parameter estimate, $\Delta = \frac{4}{100}$, and $M = 100$. The true parameters are chosen so that the power is one and the kurtosis is either $\beta_2 = 3.5$, 4, 5, 6, or 7. The average p-value and CDF error from 1000 trials are tabulated when $n = 200$, 500, and 1000 samples are used to estimate the parameters in Tables 1 and 2 respectively. The MLE for the log-normal data has a higher average KS statistic p-value and a lower average error than the MME for all values of β_2 and n. For the Weibull data the MLE always had smaller average error than the MME; however, the MME yielded a larger average p-value at lower values of β_2. In the remainder of this report the MME is used to estimate the parameters of the Weibull distribution and the MLE is used to estimate the parameters of the log-normal distribution.

3.4 Choosing the model with the best fit

Choosing a model to represent observed reverberation entails estimating the parameters of each of the candidate CDFs and forming an error measure between the observed data and the fitted model. As previously mentioned, there are many reasonable error measures depending on how the reverberation model is to be used. To evaluate the flexibility and accuracy of the models in representing different types of non-Rayleigh reverberation, KS statistic p-values are considered when the observed data are Rayleigh, log-normal, Weibull, K, and two component Rayleigh mixture distributed. The parameters for the source distributions were chosen so the power was one, $\beta_2 = 4.5$, and for the two component Rayleigh mixture $\epsilon = 0.9$. This places all of the models except for the Rayleigh on a vertical line in the (β_2, β_1) plane shown in Fig. 1. The data from each source distribution were fitted using Rayleigh, Edgeworth, log-normal, Weibull, K, and two and three component Rayleigh mixture models. The average p-values from 1000 trials using $n = 1000$ and $n = 200$ source data samples are shown in Figs. 2 and 3 respectively. The average errors (as defined in eq. (74)) between the actual CDF and the frequency curves (i.e., the CDF formed from the parameter estimates) are shown in Tables 3 and 4.

The Rayleigh distribution is a special case of the Edgeworth, Weibull, K, and Rayleigh mixture models. Thus, each of these models provides a good fit to a Rayleigh source distribution as seen in Figs. 2 and 3. However, the Rayleigh model results in the smallest average error between the actual CDF and the frequency curve formed from the parameter estimates as seen in Tables 3 and 4. This in fact holds for each of the generating distributions; that is, the model representing the true distribution for the data yields the minimum error. Note, however, that the

Table 1 *Average KS statistic p-values from 1000 trials for Weibull and log-normal data with samples of size $n = 200$, $n = 500$, and $n = 1000$.*

		Weibull			Log-normal		
	β_2	$n = 200$	$n = 500$	$n = 1000$	$n = 200$	$n = 500$	$n = 1000$
MLE	3.5	0.837	0.825	0.811	0.832	0.813	0.804
MME	3.5	0.854	0.842	0.832	0.829	0.813	0.802
MLE	4	0.837	0.825	0.811	0.840	0.825	0.813
MME	4	0.852	0.839	0.829	0.837	0.820	0.810
MLE	5	0.842	0.823	0.821	0.832	0.813	0.804
MME	5	0.844	0.825	0.822	0.820	0.803	0.792
MLE	6	0.842	0.823	0.821	0.841	0.811	0.816
MME	6	0.830	0.813	0.807	0.818	0.786	0.792
MLE	7	0.842	0.823	0.821	0.840	0.825	0.813
MME	7	0.830	0.813	0.807	0.816	0.800	0.783

Table 2 *Average error between estimated and actual CDF from 1000 trials for Weibull and log-normal data with samples of size $n = 200$, $n = 500$, and $n = 1000$.*

		Weibull			Log-normal		
	β_2	$n = 200$	$n = 500$	$n = 1000$	$n = 200$	$n = 500$	$n = 1000$
MLE	3.5	8.81e-04	3.43e-04	1.75e-04	3.00e-04	1.20e-04	6.04e-05
MME	3.5	8.91e-04	3.49e-04	1.78e-04	3.05e-04	1.23e-04	6.16e-05
MLE	4	9.46e-04	3.69e-04	1.88e-04	4.13e-04	1.67e-04	7.90e-05
MME	4	9.63e-04	3.79e-04	1.94e-04	4.27e-04	1.73e-04	8.13e-05
MLE	5	1.01e-03	4.26e-04	2.06e-04	5.40e-04	2.16e-04	1.09e-04
MME	5	1.04e-03	4.37e-04	2.12e-04	5.76e-04	2.33e-04	1.17e-04
MLE	6	1.04e-03	4.42e-04	2.14e-04	5.95e-04	2.49e-04	1.20e-04
MME	6	1.10e-03	4.61e-04	2.23e-04	6.58e-04	2.77e-04	1.33e-04
MLE	7	1.04e-03	4.42e-04	2.14e-04	6.44e-04	2.60e-04	1.23e-04
MME	7	1.10e-03	4.61e-04	2.23e-04	7.11e-04	2.90e-04	1.37e-04

three component Rayleigh mixture produced a slightly smaller error than the two component mixture, most likely due to a lack of convergence in the EM algorithm (200 iterations were performed for each estimate). Unfortunately, the true model does not always produce the highest average p-value as seen in Figs. 2 and 3 for the Rayleigh source distribution where the Weibull model has a better fit and for the Weibull and K source distributions where the three component Rayleigh mixture has a better fit.

Comparing Figs. 2 and 3 it is seen that when only 200 data samples are used to estimate the parameters and form the KS statistic higher p-values are observed. As shown in Table 4, this comes with an associated increase in the error.

Both Figs. 2 and 3 show that the log-normal source data is only well modelled by the log-normal distribution while the three component Rayleigh mixture represents well all of the other distributions. The generality of the Rayleigh mixture leads one to expect that it should also work well for the log-normal distribution. However, it was observed that when all of the powers are equally

$$\hat{\lambda}_i = \frac{1}{n} \sum_{j=1}^{n} X_j \tag{75}$$

for $i = 1, \ldots, m$, a maximum point is obtained when the data are log-normal distributed as opposed to a saddle point for the other distributions. Thus, the EM algorithm converges on this point resulting in a single Rayleigh with the power described in eq. (75).

Of all the CDF models considered, the three component Rayleigh mixture shows the most flexibility in fitting the data in terms of a high KS statistic p-value and a reasonable CDF error as compared to the model with minimum error.

Table 3 *Average error between estimated and actual CDF from 1000 trials for various source distributions with data samples of size $n = 1000$. The non-Rayleigh data were generated with unit power, $\beta_2 = 4.5$, and for the two component Rayleigh mixture, $\epsilon = 0.9$.*

Model	Source Distribution				
	Rayleigh	Log-norm.	Weibull	K	Mixt-2
Rayleigh	**1.190e-04**	2.302e-02	8.704e-03	1.818e-03	4.283e-04
Edgeworth	1.530e-04	1.361e-02	1.723e-03	3.086e-04	3.561e-04
Log-normal	4.401e-03	**9.341e-05**	5.721e-03	3.011e-03	3.684e-03
Weibull	1.689e-04	1.720e-03	**2.034e-04**	3.106e-04	2.842e-04
K	1.440e-04	2.302e-02	2.667e-02	**1.740e-04**	2.059e-04
Ray Mix-2	1.383e-04	2.302e-02	6.145e-04	2.054e-04	1.808e-04
Ray Mix-3	1.419e-04	2.302e-02	2.958e-04	2.072e-04	**1.747e-04**

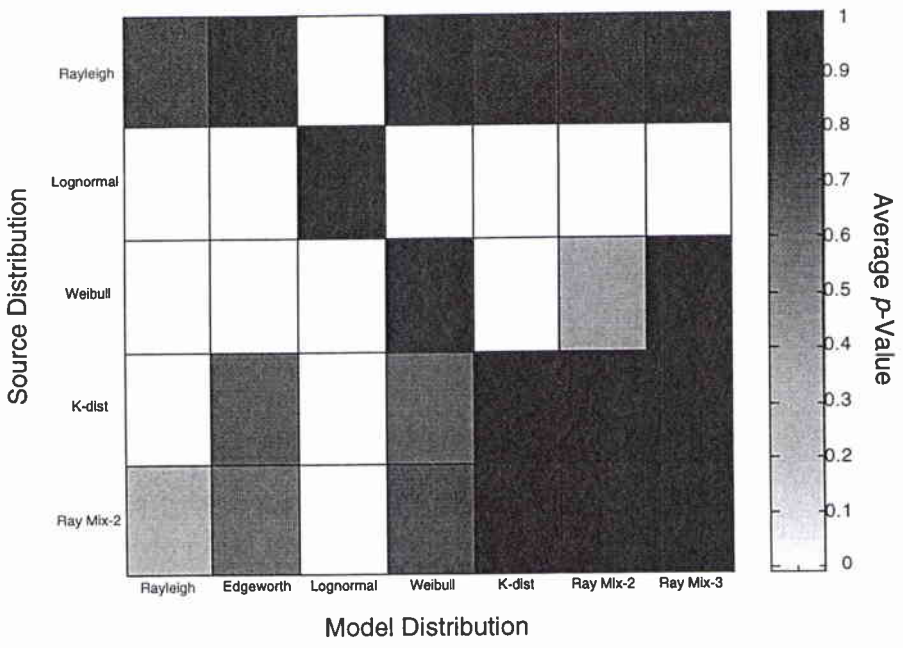

Figure 2 *Average KS statistic p-value from 1000 trials for various source distributions with data samples of size $n = 1000$. The non-Rayleigh data were generated with unit power, $\beta_2 = 4.5$, and for the two component Rayleigh mixture, $\epsilon = 0.9$.*

Table 4 *Average error between estimated and actual CDF from 1000 trials for various source distributions with data samples of size $n = 200$. The non-Rayleigh data were generated with unit power, $\beta_2 = 4.5$, and for the two component Rayleigh mixture, $\epsilon = 0.9$.*

Model	Source Distribution				
	Rayleigh	Log-norm.	Weibull	K	Mixt-2
Rayleigh	**5.676e-04**	2.328e-02	9.438e-03	2.338e-03	1.001e-03
Edgeworth	7.414e-04	1.383e-02	3.298e-03	1.436e-03	1.263e-03
Log-normal	5.070e-03	**4.884e-04**	6.432e-03	3.702e-03	4.294e-03
Weibull	8.231e-04	2.143e-03	**9.983e-04**	9.817e-04	9.893e-04
K	6.838e-04	2.328e-02	1.327e-01	**8.377e-04**	8.370e-04
Ray Mix-2	6.996e-04	2.328e-02	1.713e-03	9.312e-04	**8.086e-04**
Ray Mix-3	7.153e-04	2.328e-02	1.332e-03	9.379e-04	8.146e-04

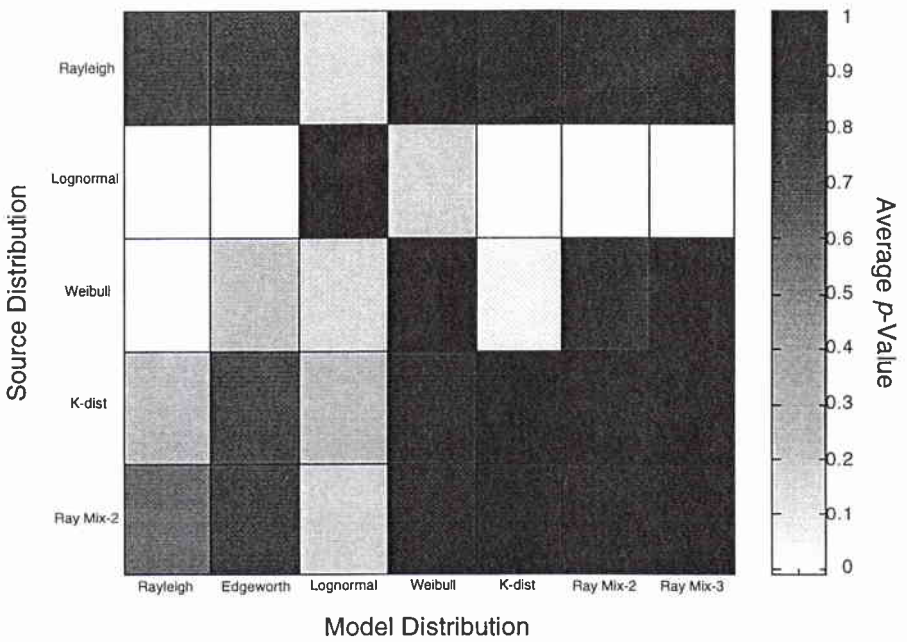

Figure 3 *Average KS statistic p-value from 1000 trials for various source distributions with data samples of size $n = 200$. The non-Rayleigh data were generated with unit power, $\beta_2 = 4.5$, and for the two component Rayleigh mixture, $\epsilon = 0.9$.*

4

Real data example

Crucial to the statistical analysis of reverberation is the appropriate processing of the observed data. Sensor level data must be beamformed, matched filtered, base-banded, low-pass filtered, and decimated. As most of these operations are linear, the order is somewhat arbitrary. However, it is important that the quadrature and in-phase components of the matched filter output be obtained and that statistically independent samples be used to estimate the CDF. The former requires basebanding the data by the center frequency of the transmitted pulse and low-pass filtering with a cut-off frequency equal to half the bandwidth of the transmitted pulse. The latter requires decimation of the data so that the sampling rate is equal to the bandwidth of the transmitted pulse. In certain cases the data may need further processing to remove time varying scale factors.

4.1 Reverberation analysis

Once the data have been segmented so that a stationary sample is being considered, the skewness and kurtosis should be estimated and displayed on a (β_2, β_1) plane similar to that of Fig. 1. This will provide an idea of which distributions should be considered for modeling the observed data. For instance, the Edgeworth series and K distributions will not model reverberation with lighter tails (i.e., smaller kurtosis) than the Rayleigh distribution. This process is illustrated in Fig. 4 where (β_2, β_1) estimates from several data sets are displayed. Clearly real reverberation data can vary from being Rayleigh distributed to log-normal, Weibull, or K-distributed. As many researchers have shown, much of the variation can be described by system parameters such as grazing angle and overall transmit-receive beamwidths, signal duration and bandwidth.

The parameter estimates of the candidate analytical CDFs are then formed from the observed data and used to generate the KS statistics. For example, consider some long-range low-frequency active sonar (LFAS) reverberation. KS statistics formed from adjacent segments each containing 1000 samples from one ping of data are shown in Table 5 where it is seen that either the three or four component Rayleigh mixture provides the best fit. Parameter estimates formed from 5000 data points are used to approximate the probability of false alarm, as shown in Fig. 5. Here it is seen that only the Rayleigh mixture has the flexibility to model the shape for moderate

threshold values (i.e., < 2) and still produce reasonable tails. A disadvantage of this flexibility is that the Rayleigh mixture may not provide accurate modeling where there is little or no observed data, as seen in the tails of the distribution. Note, however, that other models will suffer similarly if they are not based on the underlying physical phenomenon.

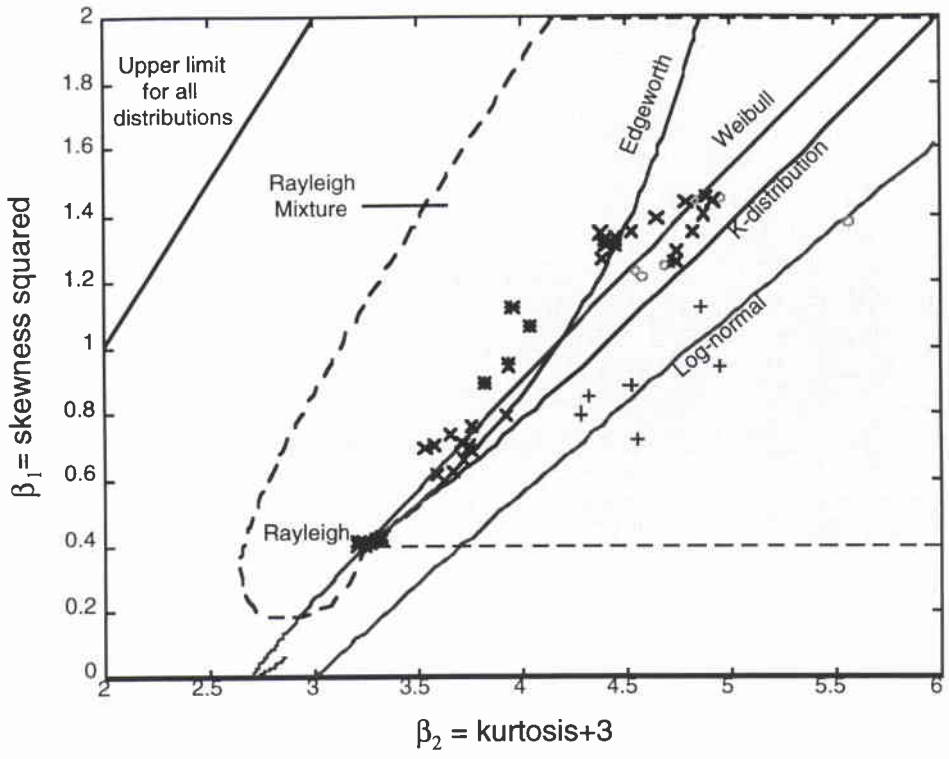

Figure 4 *(β_2, β_1) plane with real data: narrow transmit beam parametric sonar (+), wide transmit beam parametric sonar (○), high frequency bottom backscatter data from an omni-directional receiver with a 20 degree transmitter beamwidth for various grazing angles and bottom types (×), long-range low-frequency active sonar reverberation (∗).*

Table 5 *KS statistic p-values from fitting 5 samples of 1000 data points from one ping of LFAS data. In each case, the three or four component Rayleigh mixture provides the best fit.*

Rayleigh	Edgew.	Log-norm.	Weibull	K	Mixt-2	Mixt-3	Mixt-4
1.1e-22	5.0e-11	3.8e-14	0.132	0.003	0.013	**0.554**	0.545
5.9e-21	8.2e-06	6.2e-10	0.584	0.028	0.034	0.445	**0.690**
2.5e-31	4.8e-11	1.4e-13	0.291	0.010	0.112	0.774	**0.991**
1.3e-19	7.5e-11	8.3e-14	0.127	0.003	0.060	**0.696**	0.525
7.3e-26	2.1e-09	3.1e-12	0.224	0.005	0.084	0.767	**0.928**

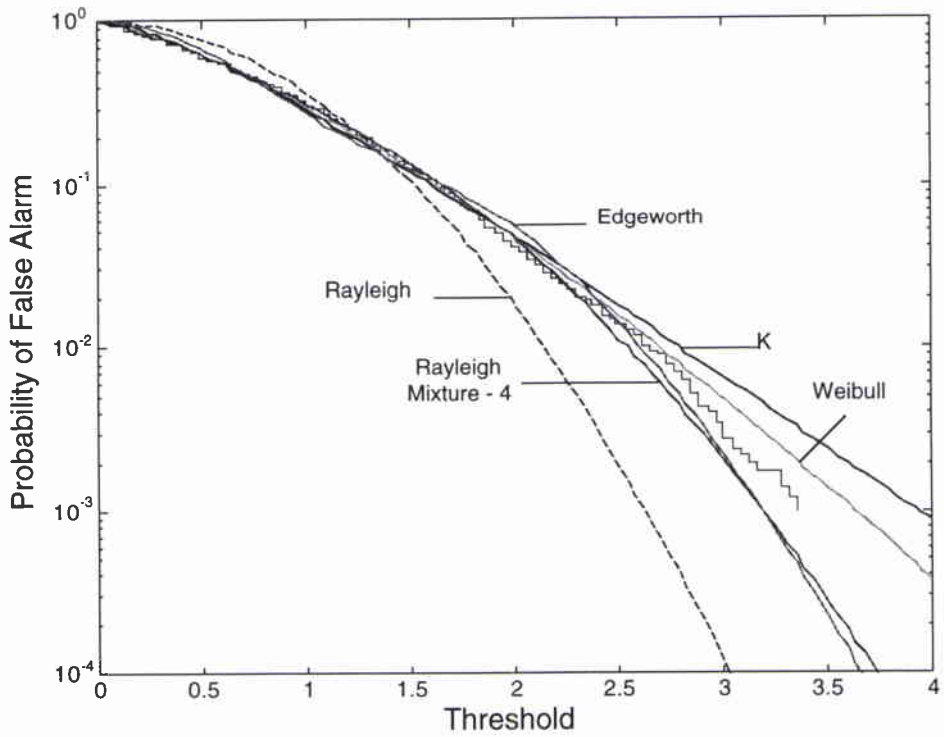

Figure 5 *Fitted and estimated probability of false alarm for LFAS data. The Rayleigh mixture with four components provide the best overall fit.*

4.2 Theoretical ROC curves

As previously mentioned, the K and Rayleigh mixture distributions are well suited to representing target models within non-Rayleigh reverberation. The Rayleigh mixture is particularly easy to deal with as described in Section 2.6. The mixture proportions and powers estimated from the LFAS data in the previous section are used here to generate theoretical ROC curves assuming a non-fluctuating target (i.e., deterministic or Swerling type zero). When the signal is present, the magnitude matched filter output is a mixture of Rician random variables with scale parameters λ_i and non-centrality parameters $\delta_i = 2\frac{\gamma}{\lambda_i}$, resulting in the CDF

$$F(x) = \sum_{i=1}^{m} \epsilon_i F_r(x; \lambda_i, \delta_i) \tag{76}$$

where $F_r(x; \lambda, \delta)$ is the Rician CDF

$$F_r(x; \lambda, \delta) = \int_{y=0}^{x} \frac{y}{\lambda} \mathrm{e}^{-\frac{1}{2}\left(\delta + \frac{y^2}{\lambda}\right)} \mathrm{I}_0\left(y\sqrt{\frac{\delta}{\lambda}}\right) dy. \tag{77}$$

Here γ represents the power in the signal and $\mathrm{I}_0(x)$ is the zero-order modified Bessel function. The Rician CDF may be evaluated using the three-moment approximation recommended by Johnson, Kotz, and Balakrishnan [35] for the noncentral chi-squared distribution as a noncentral chi-squared random variable with two degrees of freedom is the square of a Rician random variable. Figure 6 contains theoretical ROC curves when the signal power (and also the signal-to-reverberation ratio (SRR) as the total reverberation power is one) is 5, 10, and 13 dB for the Rayleigh mixture estimated from the LFAS data and for standard Rayleigh reverberation. It is clear that the heavy tails of the non-Rayleigh reverberation adversely affect detection performance. Except for low threshold (i.e., high probability of false alarm) there can be a significant drop in detection probability between Rayleigh and non-Rayleigh reverberation. At lower thresholds, which are not particularly of interest, detection performance is slightly better for the non-Rayleigh reverberation background because of the smaller probability of a false alarm compared to the Rayleigh reverberation which is also seen in Fig. 5.

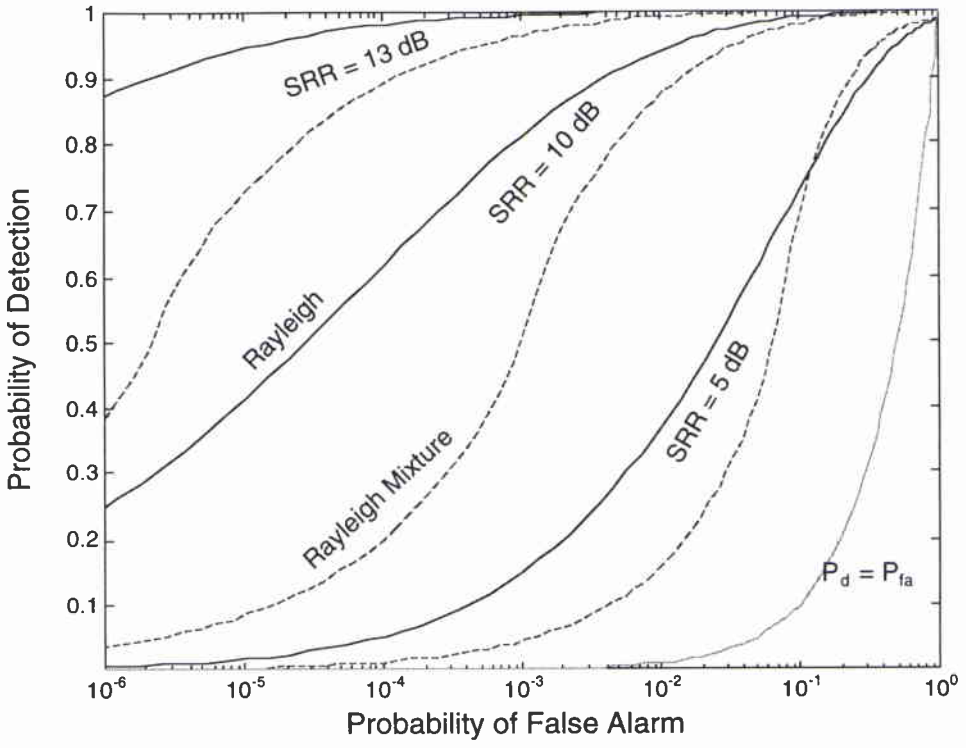

Figure 6 *Theoretical ROC curves based on Rayleigh reverberation (solid lines) and the Rayleigh mixture model (dashed lines) with parameters estimated from real data.*

5 Conclusion

This report has presented several common models for non-Rayleigh reverberation along with the means to estimate their parameters. Of these models, the Edgeworth expansion, Weibull, K, and Rayleigh mixtures have as a member the traditional Rayleigh distribution. The K and Rayleigh mixture models are additionally able to account for the presence of a target using standard models such as those of Swerling, thus allowing examination of theoretical ROC curves or the implementation of more appropriate detectors.

An analysis technique for choosing which non-Rayleigh reverberation model best fits observed data was proposed. This consisted of first evaluating the skewness and kurtosis (via β_1 and β_2) of observed data to provide initial guidance toward choosing which of the reverberation models are appropriate. The Kolmogorov-Smirnov statistic, a non-parametric measure of the error between the sample CDF and the model CDF, is then used to choose the model with the best fit. Simulation analysis indicated that if one model is to be chosen to represent a wide variety of non-Rayleigh distributions, the Rayleigh mixture provides the most flexibility. The exception to this conclusion is that the Rayleigh mixture CDF formed from the maximum likelihood parameter estimates does not approximate well the log-normal CDF, which seems to arise when a narrow beam [2] or parametric [5] sonar is used. Real data were used to demonstrate this analysis process, including examination of theoretical ROC curves formed from the reverberation CDF estimated from the data. Here it was seen that the heavier tails of non-Rayleigh reverberation adversely affect detection performance compared to the Rayleigh reverberation.

Matlab subroutines created for parameter estimation, CDF and PDF evaluation, and random number generation are included in Annex B.

Acknowledgements

The author thanks Warren Fox for providing parametric sonar data, Ettore Capriulo for providing LFAS data, and Anthony Lyons for instigating this work, providing high frequency bottom backscatter data, and many helpful discussions.

References

Sonar references

[1] D. Alexandrou, C. de Moustier, and G. Haralabus, "Evaluation and verification of bottom acoustic reverberation statistics predicted by the point scattering model," *Journal of the Acoustical Society of America*, vol. 91, no. 3, pp. 1403–1413, March 1992.

[2] N. P. Chotiros *et al.*, "Acoustic backscattering at low grazing angles from the ocean bottom. Part II. Statistical characteristics of bottom backscatter at a shallow water site," *Journal of the Acoustical Society of America*, vol. 77, no. 3, pp. 975–982, March 1985.

[3] P. A. Crowther, *Fluctuation Statistics of Sea-bed Acoustic Backscatter*, pp. 609–622, Plenum, New York, 1980.

[4] P. Faure, "Theoretical model of reverberation noise," *Journal of the Acoustical Society of America*, vol. 36, no. 2, pp. 259–266, February 1964.

[5] M. Gensane, "A statistical study of acoustic signals backscattered from the sea bottom," *IEEE Journal of Oceanic Engineering*, vol. 14, no. 1, pp. 84–93, January 1989.

[6] D. Marandino, "Low-frequency reverberation measurements with an activated towed array: Scattering strengths and statistics," SR-112, SACLANT Undersea Research Centre, 1987.

[7] S. T. McDaniel, "Seafloor reverberation fluctuations," *Journal of the Acoustical Society of America*, vol. 88, no. 3, pp. 1530–1535, September 1990.

[8] V. V. Ol'shevskii, *Characteristics of Sea Reverberation*, Consultants Bureau, New York, 1967.

[9] S. Stanic and E. G. Kennedy, "Fluctuations of high-frequency shallow-water seafloor reverberation," *Journal of the Acoustical Society of America*, vol. 91, no. 4, pp. 1967–1973, April 1992.

[10] S. Stanic and E. G. Kennedy, "Reverberation fluctuations from a smooth seafloor," *IEEE Journal of Oceanic Engineering*, vol. 18, no. 2, pp. 95–99, April 1993.

[11] W. K. Stewart, D. Chu, S. Malik, S. Lerner, and H. Singh, "Quantitative seafloor characterization using a bathymetric sidescan sonar," *IEEE Journal of Oceanic Engineering*, vol. 19, no. 4, pp. 599–610, October 1994.

[12] G. R. Wilson and D. R. Powell, "Probability density estimates of surface and bottom reverberation," *Journal of the Acoustical Society of America*, vol. 73, no. 1, pp. 195–200, January 1983.

Radar references

[13] B. C. Armstrong and H. D. Griffiths, "CFAR detection of fluctuating targets in spatially correlated K-distributed clutter," *IEE Proceedings-F, Radar and Signal Processing*, vol. 138, no. 2, pp. 139–152, April 1991.

[14] E. Conte, M. Longo, and M. Lops, "Modeling and simulation of non-Rayleigh radar clutter," *IEE Proceedings-F, Radar and Signal Processing*, vol. 138, no. 2, pp. 121–130, April 1991.

[15] E. Conte, M. Longo, and M. Lops, "Radar detection of signals with unknown parameters in K-distributed clutter," *IEE Proceedings-F, Radar and Signal Processing*, vol. 138, no. 2, pp. 131–138, April 1991.

[16] T. Hair, T. Lee, and C. J. Baker, "Statistical properties of multifrequency high-range-resolution sea reflections," *IEE Proceedings-F, Radar and Signal Processing*, vol. 138, no. 2, pp. 75–79, April 1991.

[17] M. Jahangir, D. Blacknell, and R. G. White, "Accurate approximation to the optimum parameter estimate for K-distributed clutter," *IEE Proceedings - Radar, Sonar and Navigation*, vol. 143, no. 6, pp. 383–390, December 1996.

[18] E. Jakeman and P. N. Pusey, "A model for non-Rayleigh sea echo," *IEEE Transactions on Antennas and Propagation*, vol. 24, no. 6, pp. 806–814, 1976.

[19] P. Lombardo and C. J. Oliver, "Estimation of texture parameters in K-distributed clutter," *IEE Proceeedings - Radar, Sonar and Navigation*, vol. 141, no. 4, pp. 196–204, August 1994.

[20] R. S. Raghavan, "A method for estimating parameters of K-distributed clutter," *IEEE Transactions on Aerospace and Electronic Systems*, vol. 27, no. 2, pp. 238–246, March 1991.

[21] G. V. Trunk, "Non-Rayleigh sea clutter: Properties and detection of targets," Report 7986, Naval Research Laboratory, 1976, Reprinted in *Automatic Detection and Radar Data Processing*, D. C. Schleher, Ed., Artech House, Dedham, 1980.

[22] K. D. Ward, "Compound representation of high resolution sea clutter," *Electronics Letters*, vol. 17, no. 16, pp. 561–563, August 1981.

[23] K. D. Ward, "Compound representation of high resolution sea clutter," in *IEE Conference Publication 216 (Radar-82)*, 1982, pp. 203–207.

[24] S. Watts, "Radar detection prediction in sea clutter using the compound K-distribution model," *IEE Proceedings-F, Radar and Signal Processing*, vol. 132, no. 7, pp. 613–620, December 1985.

Miscellaneous references

[25] P. P. Gandhi and S. A. Kassam, "Analysis of CFAR processors in nonhomogenous background," *IEEE Transactions on Aerospace and Electronic Systems*, vol. 24, no. 4, pp. 427–445, July 1988.

[26] E. Jakeman and R. J. A. Tough, "Non-Gaussian models for the statistics of scattered waves," *Advances in Physics*, vol. 37, no. 5, pp. 471–529, 1988.

[27] I. R. Joughin, D. B. Percival, and D. P. Winebrenner, "Maximum likelihood estimation of K distribution parameters for SAR data," *IEEE Transactions on Geoscience and Remote Sensing*, vol. 31, no. 5, pp. 989–999, September 1993.

[28] J. A. Ritcey, S. D. Gordon, and T. E. Ewart, "A probability distribution for the complex field of waves propagating in random media," *Journal of the Acoustical Society of America*, vol. 100, no. 1, pp. 237–244, July 1996.

Mathematic and statistical references

[29] H. Akaike, "A new look at the statistical model identification problem," *IEEE Transactions on Automatic Control*, pp. 716–723, December 1974.

[30] A. P. Dempster, N. M. Laird, and D. B. Rubin, "Maximum likelihood from incomplete data via the EM algorithm," *Journal of the Royal Statistical Society, Series B*, vol. 2, pp. 1–38, 1977.

[31] M. Fisz, *Probability Theory and Mathematical Statistics*, John Wiley & Sons, Inc., third edition, 1963.

[32] R. V. Hogg and A. T. Craig, *Introduction to Mathematical Statistics*, Macmillan Pub. Co., New York, fourth edition, 1978.

[33] Johnson and Kotz, Eds., *Encylcopedia of Statistical Sciences*, vol. 3, John Wiley & Sons, Inc., 1983.

[34] N. L. Johnson, S. Kotz, and N. Balakrishnan, *Continuous Univariate Distributions*, vol. 1, John Wiley & Sons, Inc., second edition, 1994.

[35] N. L. Johnson, S. Kotz, and N. Balakrishnan, *Continuous Univariate Distributions*, vol. 2, John Wiley & Sons, Inc., second edition, 1995.

[36] E. L. Lehmann, *Theory of Point Estimation*, John Wiley & Sons, Inc., 1983.

[37] B. W. Lindgren, *Statistical Theory*, Macmillan Pub. Co., New York, third edition, 1976.

[38] G. J. McLachlan and K. E. Basford, *Mixture Models, Inference and Applications to Clustering*, Marcel Dekker, Inc., 1988.

[39] L. Råde and B. Westergren, *Beta β Mathematics Handbook*, CRC Press, Boca Raton, Florida, second edition, 1990.

[40] R. A. Redner and H. F. Walker, "Mixture densities, maximum likelihood and the EM algorithm," *SIAM Review*, vol. 26, no. 2, April 1984.

[41] J. Rissanen, "Modeling by shortest data description," *Automatica*, pp. 465–471, September 1978.

[42] J. Spanier and K. B. Oldham, *An Atlas of Functions*, Hemisphere Pub. Corp., Washington, 1987.

[43] M. A. Tanner, *Tools for Statistical Inference: Methods for the Exploration of Posterior Distributions and Likelihood Functions*, Springer-Verlag, New York, second edition, 1993.

[44] D. M. Titterington, A. F. M. Smith, and U. E. Makov, *Statistical Analysis of Finite Mixture Distributions*, John Wiley & Sons, Inc., Chichester, 1985.

Annex A

Skewness and kurtosis for non-Rayleigh distributions

The information required to compute the skewness and kurtosis (more specifically, β_1 and β_2) for the Edgeworth expansion, log-normal, Weibull, and two component Rayleigh mixture distributions is presented in this annex along with the means to create the boundary of the two component Rayleigh mixture region in the (β_2, β_1) plane of Fig. 1.

The Edgeworth series has been applied here to the quadrature and in-phase components of the matched filter output with a restriction that the PDF be symmetric about zero which results in zero skewness. This does not imply that the skewness of the matched filter magnitude is zero. The Edgeworth series PDF is a two parameter model which results in a line on the (β_2, β_1) plane. The moments of the Edgeworth series may be found by appropriately integrating the PDF presented in eq. (7),

$$\mathrm{E}[X] = \frac{\sqrt{\lambda\pi}}{2}\left(1 - \frac{\gamma}{32} - \frac{5\gamma^2}{8192}\right), \tag{78}$$

$$\mathrm{E}\left[X^2\right] = \lambda, \tag{79}$$

$$\mathrm{E}\left[X^3\right] = \frac{3\lambda^{\frac{3}{2}}\sqrt{\pi}}{4}\left(1 + \frac{3\gamma}{32} + \frac{3\gamma^2}{8192}\right), \tag{80}$$

and

$$\mathrm{E}\left[X^4\right] = \lambda^2\frac{(\gamma+4)}{2}. \tag{81}$$

The skewness and kurtosis (or equivalently β_1 and β_2) are easily found by relating the non-central moments ($\alpha_i = \mathrm{E}[X^i]$) to the central ones ($\mathrm{E}\left[(X-\mu)^i\right]$),

$$\beta_1 = \frac{\left(\alpha_3 - 3\alpha_1\alpha_2 + 2\alpha_1^3\right)^2}{\left(\alpha_2 - \alpha_1\right)^3} \tag{82}$$

and

$$\beta_2 = \frac{\alpha_4 - 4\alpha_1\alpha_3 + 6\alpha_1^2\alpha_2 - 3\alpha_1^4}{\left(\alpha_2 - \alpha_1\right)^2}. \tag{83}$$

The log-normal distribution with the PDF presented in eq. (11) results in [34]

$$\beta_1 = (w-1)(w+2)^2 \tag{84}$$

and

$$\beta_2 = w^4 + 2w^3 + 3w^2 - 3 \tag{85}$$

where

$$w = \mathrm{e}^{\frac{1}{\alpha^2}}. \tag{86}$$

The Weibull PDF of eq. (24) results in the moments

$$\mathrm{E}\left[X^i\right] = \alpha^{-\frac{i}{\beta}}\Gamma\left(1+\frac{i}{\beta}\right) \tag{87}$$

from which the skewness and kurtosis may be derived using eqs. (82) and (83). The moments of the K-distribution, as described in eq. (46), may be similarly used.

The moments of a two component Rayleigh mixture are

$$\begin{aligned}\mathrm{E}\left[X^i\right] &= (1-\epsilon)\lambda_0^{\frac{i}{2}}\Gamma\left(1+\frac{i}{2}\right) + \epsilon\lambda_1^{\frac{i}{2}}\Gamma\left(1+\frac{i}{2}\right) \\ &= \lambda_0^{\frac{i}{2}}\Gamma\left(1+\frac{i}{2}\right)\left(1-\epsilon+\epsilon\Delta^{\frac{i}{2}}\right)\end{aligned} \tag{88}$$

where $\Delta = \frac{\lambda_1}{\lambda_0}$. These may be used as noted above to form the skewness and kurtosis. Varying $\epsilon \in [0,1]$ and $\Delta \in (0,\infty)$ results in the region shown in Fig. 1. The curved boundary starting from the Rayleigh point and moving clockwise (i.e., southwest then curving around to north) is obtained by letting $\Delta \to 0$ when $\epsilon \in (0,1)$. This results in the moments

$$\mathrm{E}\left[X^i\right] = \lambda_0^{\frac{i}{2}}\Gamma\left(1+\frac{i}{2}\right)(1-\epsilon) \tag{89}$$

which may be used to produce β_1 and β_2 via eqs. (82) and (83). The boundary moving directly east from the Rayleigh point is obtained by letting $\epsilon \to 0$ and $\Delta \to \infty$ in such a manner that $\epsilon\Delta^{1.5} \to 0$ and $\epsilon\Delta^2 \to \infty$. This results in

$$\beta_1 = \frac{4\pi(\pi-3)^2}{(4-\pi)^3} \tag{90}$$

which is identical to β_1 for a single Rayleigh random variable, and

$$\beta_2 = \frac{32 - 3\pi^2 + 32\epsilon\Delta^2}{(4-\pi)^2} \tag{91}$$

which increases with $\epsilon\Delta^2$.

Annex B

Matlab subroutines

B.1 Rayleigh

B.1.1 Probability density function

```
function p = raylpdf(x,a)
%RAYLPDF Rayleigh probability distribution function (pdf).
% P = RAYLPDF(X,A) returns the Rayleigh pdf with power A at the values in X.
p=2*x.*exp(-(x.^2)/a)/a;
```

B.1.2 Cumulative distribution function

```
function p = raylcdf(x,a,b)
%RAYLCDF Rayleigh cumulative distribution function (cdf).
% P = RAYLCDF(X,A) returns the Rayleigh cdf with power A at the values in X.
p=1-exp(-(x.^2)/a);
```

B.1.3 Statistics

```
function [a1,var,sk,kurt]= raylstat(a)
% [MN,VAR,SK,KURT] = RAYLSTAT(A) returns the mean, variance,
% skewness and kurtosis of the Rayleigh distribution with power A.
a1=sqrt(pi*a)/2;
var=a*(1-pi/4);
sk=ones(size(a))*2*sqrt(pi)*(pi-3)/((4-pi)^(3/2));
kurt=ones(size(a))*(32-3*pi^2)/((4-pi)^2)-3;
```

B.1.4 Random number generation

```
function r=raylrnd(v,n,m)
% r=RAYLRND(P,n,m)
% Returns a matrix of Rayleigh random variables  with power P
if (nargin==1),
  r=weibrnd(1../v,2);
elseif (nargin==2),
  r=weibrnd(1../v,2,n,1);
elseif (nargin==3),
  r=weibrnd(1../v,2,n,m);
end;
```

B.2 Edgeworth expansion

B.2.1 Probability density function

```
function y = edgepdf(x,a,b)
%EDGEPDF Edgeworth expansion probability density function (cdf).
% Y = EDGEPDF(X,A,B) Returns the Edgeworth expansion pdf with
% parameters A and B at the values in X.  Note, A and B must be scalars.
% The parameters A and B are related to the moments of x as follows:
%    E[X^2] = A
%    E[X^4] = A^2 (B+4)/2
y = zeros(size(x));
% The domain of the K-distribution is the positive real axis.
k = find(x > 0);
if any(k),
  z=(x(k).^2)/a;
  c=b/24;
  y(k)=(2/a)*x(k).*exp(-z).*(1+c*(3*(z.^2)-12*z+6)+...
       c*c*(3*(z.^4)/8-6*(z.^3)+27*(z.^2)-36*z+9));
end;
```

B.2.2 Cumulative distribution function

```
function y = edgecdf(x,a,b)
%EDGECDF Edgeworth expansion cumulative density function (cdf).
% Y = EDGECDF(X,A,B) Returns the Edgeworth expansion cdf with
% parameters A and B at the values in X.  Note, A and B must be scalars.
y = zeros(size(x));
% The domain of the K-distribution is the positive real axis.
k = find(x > 0);
if any(k),
  z=(x(k).^2)/a;
  ez=exp(-z);
  y(k)=(1-ez)-(b/64)*z.*ez.*(b*(z.^3)/24-b*(z.^2)/2+(3*b+16)*z/2-b-16);
end;
```

B.2.3 Statistics

```
function [a1,var,sk,kurt]= edgestat(a,g);
% [MN,VAR,SK,KURT] = EDGESTAT(A,G) returns the mean, variance,
% skewness and kurtosis of the Edgeworth approximation with
% parameters A and G.
a1=sqrt(a*pi)/2.*(1-(g/32)-5*(g.^2)/8192);
a2=a;
a3=3*a.*sqrt(a*pi)*(1+(3*g/32)+3*(g.^2)/8192)/4;
a4=(a.^2).*(g+4)/2;
var=a2-a1.^2;
sk=(a3-3*a1.*a2+2*(a1.^3))./(var.^(3/2));
kurt=(a4-4*a1.*a3+6*(a1.^2).*a2-3*(a1.^4))./(var.^2)-3;
```

B.2.4 Method of moments estimator

```
function [a,b] = edgemme(x)
%EDGEMME Edgeworth expansion method of moments parameter estimation.
% [A,B] = EDGEMME(X) Returns the parameter estimates for the
% Edgeworth expansion pdf from the amplitude data X.
a=mean(x.^2);
b=2*mean(x.^4)./(a.^2) -4;
```

B.3 Log normal

B.3.1 Probability density function

```
function y = lognpdf(x,a,b)
%LOGNPDF Log-normal probability density function (pdf).
% Y = LOGNPDF(X,A,B) Returns the log-normal pdf with parameters A and B.
%       f(x) = a /[sqrt(2pi)x] exp{-0.5*[b+a*log(x)]^2} for x>=0
%       E[X] = exp{[1-2ab]/(2a^2)}
%       E[X^2] = exp{2[1-ab]/(a^2)}
y = zeros(size(x));
% The domain of the log-normal distribution is the positive real axis.
k = find(x > 0);
if any(k),
  y(k)=(a(k)./(sqrt(2*pi)*x(k))).*exp(-0.5*(b(k)+a(k).*log(x(k))).^2);
end;
```

B.3.2 Cumulative distribution function

```
function p = logncdf(x,a,b)
%LOGNCDF Log-normal cumulative distribution function (cdf).
% P = LOGNCDF(X,A,B) returns the log-normal cdf with parameters A and B
% at the values in X.
p = zeros(size(x));
% The domain of the log-normal distribution is the positive real axis.
k = find(x > 0);
if any(k),
  p(k) = normcdf(a(k).*log(x(k))+b(k));
end;
```

B.3.3 Statistics

```
function [mn,var,skw,kurt]= lognstat(a,b);
% [MN,VAR,SKW,KURT] = LOGNSTAT(A,B) returns the mean, variance,
% skewness and kurtosis of the log-normal distribution with parameters A and B.
mn = exp((1-2*a.*b)./(2*a.^2));
var = exp(2*(1-a.*b)./(a.^2))-(mn.^2);
w=exp(1../(a.^2));
skw=sqrt(w-1).*(w+2);
kurt=(w.^2).*(w.^2+2*w+3)-6;
```

B.3.4 Method of moments estimators

```
function [a,b]=lognmme(u,v)
% [a,b]=LOGNMME(u,v)
% Finds the method of moments estimates of the (a,b)
% parameters of the log-normal distribution matching
% the mean (u) and variance (v).
a=1/sqrt(log(1+v/(u^2)));
b=(1/(2*a))-a*log(u);
```

B.3.5 Maximum likelihood estimators

```
function [a,b] = lognmle(x)
%LOGNMLE Maximum likelihood estimator for log-normal distribution parameters
% [A,B] = LOGNMLE(X) returns the maximum likelihood estimators
% for the A and B parameters of the log-normal distribution from the values in X.
z=log(x);
uz=mean(z);
sz=sqrt(mean(z.^2)-uz^2);
a=1/sz;
b=-uz*a;
```

B.3.6 Random number generation

```
function r = lognrnd(a,b,m,n);
%LOGNRND Random matrices from log-normal distribution.
% R = LOGNRND(A,B,M,N) returns an M-by-N matrix of random numbers chosen
% from the log-normal distribution with parameters A and B.
r = zeros(m,n);
mu=-b./a;
sigma=1../a;
r = exp(randn(m,n).*sigma + mu);
```

B.4 Weibull

Subroutines for the Weibull CDF, PDF and random number generation are available from Matlab.

B.4.1 Statistics

```
function [a1,var,sk,kurt]= weibstat(a,b);
% [MN,VAR,SK,KURT] = WEIBSTAT(A,B) returns the mean, variance,
% skewness and kurtosis of the Weibull distribution with parameters A and B.
a1=a.^(-1 ./ b) .* gamma(1 + (1 ./ b));
a2=a.^(-2 ./ b) .* gamma(1 + (2 ./ b));
a3=a.^(-3 ./ b) .* gamma(1 + (3 ./ b));
a4=a.^(-4 ./ b) .* gamma(1 + (4 ./ b));
var=a2-a1.^2;
sk=(a3-3*a1.*a2+2*(a1.^3))./(var.^(3/2));
kurt=(a4-4*a1.*a3+6*(a1.^2).*a2-3*(a1.^4))./(var.^2)-3;
```

B.4.2 Method of moments estimators

```
function [a,b]=weibmme(u,v)
% [a,b]=WEIBMME(u,v)
% Finds the method of moments estimates of the (a,b)
% parameters of the Weibull distribution matching the mean (u) and variance (v).
s=(u^2)/v;
% Find b using Newton-Raphson iteration
TOL=1e-8;
err=2*TOL;
b=0.1;
c1=gamma(1+b);
c2=gamma(1+2*b);
f=c1^2/(c2-c1^2)-s;
while (err>TOL),
  d1=digamma(1+b)*c1;
  d2=digamma(1+2*b)*c2;
  fp=2*c1*(d1*c2-d2*c1)/((c2-c1^2)^2);
  b=b-f/fp;
  err=abs(f/fp);
  c1=gamma(1+b);
  c2=gamma(1+2*b);
  f=c1^2/(c2-c1^2)-s;
end;
b=1/b;
a=(gamma(1+1/b)/u)^b;
```

B.5.2 Cumulative distribution function

```
function y = kcdf(x,a,b)
%KCDF K-distribution cumulative density function (cdf).
% Y = KCDF(X,A,B) Returns the K-distribution cdf with
% parameters A and B at the values in X.  Note, A and B
% must be scalars.
y = zeros(size(x));
% The domain of the K-distribution is the positive real axis.
tmp=2*x/sqrt(a);
tmin=0.1+10.5*((b/250)^4);
k = find(tmp<=tmin);
if (any(k)),
  if (b>2),
    y(k)=1-exp((b-2)*log(1-(x(k).^2)/(a*(b-1)*(b-2))));
  elseif (b>1),
    y(k)=(x(k).^2)/(a*(b-1));
  elseif (b>0),
    y(k)=-gamma(-b)*(((x(k).^2)/a).^b)/gamma(b);
  else,
    tmin=0;
  end;
end;
k = find(tmp > tmin);
if any(k),
  y(k)=1-exp(b*log(tmp(k))+log(besselk(b,tmp(k)))-gammaln(b)-(b-1)*log(2));
end;
```

B.5.3 Statistics

```
function [a1,var,sk,kurt]= kstat(a,b);
% [MN,VAR,SK,KURT] = KSTAT(A,B) returns the mean, variance,
% skewness and kurtosis of the K-distribution with
% parameters A and B.
a1=0.5*gamma(b+0.5).*sqrt(pi*a)./gamma(b);
a2=b.*a;
a3=0.75*gamma(b+1.5).*sqrt(pi*a).*a./gamma(b);
a4=2*b.*(b+1).*(a.^2);
var=a2-a1.^2;
sk=(a3-3*a1.*a2+2*(a1.^3))./(var.^(3/2));
kurt=(a4-4*a1.*a3+6*(a1.^2).*a2-3*(a1.^4))./(var.^2)-3;
```

B.5.4 Random number generation

```
function x=krnd(a,b,n,m)
% x=KRND(a,b,n,m)
% K-distribution random number generator
x=raylrnd(a,n,m).*sqrt(gamrnd(b,1,n,m));
```

B.4.3 Maximum likelihood estimators

```
function [a,b]=weibmle(x)
% [a,b]=WEIBMLE(x)
% Finds the maximum likelihood estimates of the (a,b) parameters of
% the Weibull distributed data x using an iterative algorithm from
% Johnson & Kotz, Continuous Univariate Distributions (Vol 2, pg 41).

% Convert data to Extreme Value Distribution
z=log(x);
% Estimate scale parameter via iteration
TOL=1e-4;
err=2*TOL;
zb=mean(z);
th=-sqrt(6)*sqrt(mean((z-zb).^2))/pi;
while (err>TOL),
  w=exp(-z/th);
  th0=th;
  th=zb-sum(w.*z)/sum(w);
  err=abs((th0-th)/th);
end;
zet=-th*log(mean(exp(-z/th)));
% Convert to Johnson & Kotz parameterization of a Weibull RV
c=-1/th;
alp=exp(zet);
% Convert to matlab representation of a Weibull RV
a=1/(alp^c);
b=c;
```

B.5 K-distribution

B.5.1 Probability density function

```
function y = kpdf(x,a,b)
%KPDF K-distribution probability density function (pdf).
% Y = KPDF(X,A,B) Returns the K-distribution pdf with
% parameters A and B at the values in X.  Note, A and B
% must be scalars.
y = zeros(size(x));
% The domain of the K-distribution is the positive real axis.
k = find(x > 0);
if any(k),
  y(k)=4*((x(k)/sqrt(a)).^b).*besselk(abs(b-1),2*x(k)/sqrt(a))/(sqrt(a)*gamma(b));
end;
```

B.5.5 Method of moments estimators

```
function [a,b]=kmme(u,v)
% [a,b]=KMME(u,v)
% Finds the method of moments estimates of the (a,b)
% parameters of the K-distribution matching
% the mean (u) and variance (v).  Note that if
% s=(u^2)/v > pi/(4-pi) then the moments can not be
% matched (i.e., the tails are lighter than Rayleigh).
b=nan;
a=nan;
s=(u^2)/v;
smax=pi/(4-pi);
if (s<smax),
  % Initialize using asymptotic solution
  b=1../(4*(-log(4)+log(pi)+log(1+1../s)));
  b=max(b,0.1);
  % Hone in using Newton-Raphson iteration
  TOL=1e-8;
  err=2*TOL;
  while (err>TOL),
    % Evaluate function and derivative
    if (b<=20),
      tmp=b*(gamma(b)/gamma(b+0.5))^2;
    else,
      tmp=exp(1)*((1+1/(2*b*(12*b+7)))^2)/((1+1/(2*b))^(2*b));
    end;
    h=4*tmp/pi-1;
    hp=(4*tmp/(pi*b))*(1+2*b*(digamma(b)-digamma(b+0.5)));
    f=1/h-s;
    fp=-hp/(h^2);
    % Update estimate
    b0=b;
    b=b-f/fp;
    err=abs((b0-b)/b);
  end;
  a=(v+u^2)/b;
end;
```

B.6 Rayleigh mixture

B.6.1 Probability density function

```
function f=raymixpdf(r,p,v)
% f=RAYMIXPDF(r,p,v), Returns the PDF of a Rayleigh mixture
if (length(p)>1),
  [nr,nc]=size(r);
  r=r(:)';
  p=p(:);
  v=v(:);
  f=2*sum(((p./v)*r).*exp(-(1../v)*(r.^2)));
  f=reshape(f,nr,nc);
else,
  f=2*r.*exp(-(r.^2)/v)/v;
end;
```

B.6.2 Cumulative distribution function

```
function f=raymixcdf(r,p,v)
% F=RAYMIXCDF(r,p,v)
% Returns the CDF of a Rayleigh mixture
if (length(p)>1),
  [nr,nc]=size(r);
  r=r(:)';
  p=p(:);
  v=v(:);
  f=1-sum((p*ones(size(r))).*exp(-(1../v)*(r.^2)));
  f=reshape(f,nr,nc);
else,
  f=1-exp(-(r.^2)/v);
end;
```

B.6.3 Statistics

```
function [a1,var,sk,kurt]= raymixstat(p,v);
% [MN,VAR,SK,KURT] = RAYMIXSTAT(p,v) returns the mean, variance,
% skewness and kurtosis of the Rayleigh mixture distribution with
% parameters p and v.  If multiple evaluations are required,
% stack them into p and v matrices.
r1=sqrt(pi)/2;
r2=1;
r3=3*sqrt(pi)/4;
r4=2;
a1=sum((p.*sqrt(v)*r1)');
a2=sum((p.*v*r2)');
a3=sum((p.*(v.^(3/2))*r3)');
a4=sum((p.*(v.^2)*r4)');
var=a2-a1.^2;
sk=(a3-3*a1.*a2+2*(a1.^3))./(var.^(3/2));
kurt=(a4-4*a1.*a3+6*(a1.^2).*a2-3*(a1.^4))./(var.^2)-3;
```

B.6.4 Maximum likelihood estimators

```
function [p,v]=raymixem(r,m,pstop,p,v)
% [p,v]=RAYMIXEM(r,m,[TOL])
% [p,v]=RAYMIXEM(r,m,[Niter])
% Returns the ML estimates of the mixture parameters using EM algorithm
%    r     - Input data (MF magnitude data)
%    m     - Number of components in the mixture
%    TOL   - Optional stopping tolerance
%    Nstop - Optional number of iterations to force algorithm to do
r=r(:)';
n=length(r);
r2=r.^2;
if (nargin==2),
  TOL=1e-3;
  Nstop=inf;
else,
  if (length(pstop)==0),
TOL=1e-3;
    Nstop=inf;
  else,
    if (pstop<1),
      TOL=pstop;
      Nstop=inf;
    else,
      Nstop=pstop;
      TOL=0;
    end;
  end;
end;
% Initialize parameter estimates
if (nargin<5),
  p=ones(m,1)/m;
  i=floor(n/m);
  v=mean(reshape(r2(1:i*m),i,m))';
end;
i=0;
Nmin=min(Nstop,10);
err=max(1,TOL*2);
while(((i<Nstop)&(err>TOL))|(i<Nmin)),
  i=i+1;
  % Compute data-component probability matrix
  A=2*((p./v)*r).*exp(-(1../v)*r2);
  W=A./(ones(m,1)*sum(A));
  p0=p;
  v0=v;
  p=mean(W')';
  v=(W*r2')./(sum(W')');
  err=norm(p0-p)/norm(p)+norm(v0-v)/norm(v);
end;
```

B.6.5 Random number generation

```
function r=raymixrnd(p,v,n,m)
% r=RAYMIXRND(p,v,n,m)
% Returns a matrix of Rayleigh mixture random variables
% with proportions p and powers v
u=rand(n,m);
a=zeros(n,m);
cp=[0; cumsum(p(:))];
for i=1:length(p),
  a=a+((u>=cp(i))&(u<cp(i+1)))*sqrt(v(i));
end;
r=a.*raylrnd(1,n,m);
```

B.7 Miscellaneous

B.7.1 Kolmogorov-Smirnov statistic

```
function [p,D]=kolsm(x,cdfname,p1,p2,p3)
% [p,D]=KOLSM(x,CDFNAME,p1,p2,p3)
% Returns the Kolmogorov-Smirnoff test statistic for the input data 'x' and the
% CDF described by CDFNAME and the associated distributional parameter p1-p3.
% The output p is the p-value from the asymptotic distribution of D.
%    D = sqrt(n)*max{|F(x)-Fn(x)|}
% Sample usage:  >[p,D]=kolsm(x,'raylcdf',mean(x));
N=length(x);
xs=reshape(sort(x),N,1);
% Evaluate CDF at each point
if (nargin==2),
  F=feval(cdfname,xs);
elseif(nargin==3),
  F=feval(cdfname,xs,p1);
elseif(nargin==4),
  F=feval(cdfname,xs,p1,p2);
elseif(nargin==5),
  F=feval(cdfname,xs,p1,p2,p3);
end;
% Find the maximum absolute difference
Fn=(1:N)'/N;
D=sqrt(N)*max(abs(Fn-F));
% Find p-value
p=ks(D);
```

B.7.2 Kolmogorov-Smirnov p-value

```
function p=ks(x)
% p = KS(x)
% Returns the p-value for x from the asymptotic Kolmogorov-Smirnov
% lambda-distribution (Ref. Fisz, 1963, pg.664).  Note that
% for x<0.1, the p-value is essentially 1.
[Nr,Nc]=size(x);
x2=reshape(x.^2,1,Nr*Nc);
ox=ones(1,Nr*Nc);
Kmax=50;
ke=(2:2:Kmax)';
ko=(1:2:Kmax)';
p=2*sum(exp(-2*(ko.^2)*x2))-2*sum(exp(-2*(ke.^2)*x2));
xmin=0.1;
ind=find(x2<=xmin^2);
if any(ind),
  p(ind)=ones(size(ind));
end;
p=reshape(p,Nr,Nc);
```

B.7.3 Sample statistics subroutine

```
function [u,v,s,k]=sampstat(x)
% [u,v,s,k]=SAMPSTAT(x)
% [b1,b2]=SAMPSTAT(x)
% Returns the sample statistics estimated from the data
u=mean(x);
v=mean((x-u).^2);
s=mean((x-u).^3)/(v^(3/2));
k=mean((x-u).^4)/(v^2)-3;
if (nargout==2),
  u=s^2;
  v=k+3;
end;
```

B.7.4 Skewness-kurtosis curve

```
function skewkurt
% Program to plot the skewness-kurtosis curves
% Rayleigh
[u,v,s,k]=raylstat(1);
b1r=s.^2;
b2r=k+3;
% Weibull
b=linspace(1.25,3.5,100);
[u,v,s,k]=weibstat(1,b);
b1w=s.^2;
b2w=k+3;
% Log-normal
b=linspace(2.5,35,100);
[u,v,s,k]=lognstat(b,1);
b1n=s.^2;
b2n=k+3;
% K-distribution
b=logspace(0.15,log10(160),100);
[u,v,s,k]=kstat(1,b);
b1k=s.^2;
b2k=k+3;
% Edgeworth
b=linspace(0,2.5,100);
[u,v,s,k]=edgestat(1,b);
b1e=s.^2;
b2e=k+3;
% Maximum for all distributions
b1a=[1 2];
b2a=b1a+1;
% Rayleigh mixture
% d->0
ev=linspace(0.001,0.62,200)';
p=[1-ev zeros(size(ev))];
v=[ones(size(ev)) zeros(size(ev))];
[u,v,s,k]=raymixstat(p,v);
b1m0=s.^2;
b2m0=k+3;
% ed^(3/2) -> 0  and  ed^2 -> inf
ed=linspace(0,0.07,3);
b1m1=(2*sqrt(pi)*(pi-3)/((4-pi)^(3/2)))^2*ones(size(ed));
b2m1=(2-3*(pi^2)/16+2*ed)/((1-pi/4)^2);
% Plot
figure(1);
plot(b2r,b1r,'b*',b2w,b1w,'b-',b2n,b1n,'r-',b2k,b1k,'g-',...
     b2e,b1e,'m-',b2a,b1a,'y-',b2m1,b1m1,'g--',b2m0,b1m0,'g--');
axis([2 6 0 2]);
```

B.7.5 Digamma function

```
function y=digamma(x)
% y=DIGAMMA(x)
% Returns the digamma (psi) function
%    y = d/dx log(Gamma(x))
% Reference:  An Atlas of Functions, J. Spanier & K.B. Oldman, pg427
y=inf*ones(size(x));
ind=find(x~=0);
if any(ind),
  xx=x(ind);
  g=zeros(size(ind));
  qgo=1;
  while (qgo),
    g=g+1./xx;
    xx=xx+1;
    if (min(xx)>=5),
      qgo=0;
    end;
  end;
  y(ind)=1+(0.46./(xx.^2) -1)./(10*xx.^2);
  y(ind)=-(y(ind)./(6*xx)+1)./(2*xx) + log(xx)-g;
end;
```

Report no. changed (Mar 2006): SR-266-UU

Document Data Sheet

NATO UNCLASSIFIED

Security Classification		Project No.
NATO UNCLASSIFIED		041-3
Document Serial No.	**Date of Issue**	**Total Pages**
SR-266	May 1997	55 pp.

Author(s)

Abraham, D.A.

Title

Modeling non-Rayleigh reverberation

Abstract

Researchers over the past three decades have experimentally examined non-Rayleigh reverberation, fitted it to standard distributions such as log-normal and Weibull, developed theoretical models to explain the variation from Rayleigh, and considered new families of distributions appropriate for modeling non-Rayleigh reverberation such as the K and Rayleigh mixture.

This report draws together several of the common statistical models for non-Rayleigh reverberation. Parameter estimates for the Edgeworth expansion, log-normal, Weibull, K, and Rayleigh mixture distributions are presented and evaluated through simulation. Their ability to represent reverberation is examined using the Kolmogorov-Smirnov statistic where it was seen that the Rayleigh mixture provided the most flexibility in representing different types of non-Rayleigh reverberation. In analyzing real reverberation data, a skewness-kurtosis plane is proposed for the initial evaluation of the non-Rayleigh character providing an indication of the viability of each model. The Kolmogorov-Smirnov statistic, or some other appropriate error measure, may then be used to choose the model with the best fit to the observed reverberation. This method is demonstrated on low-frequency active sonar data where the Rayleigh mixture was seen to provide the best fit. Theoretical receiver operating characteristic (ROC) curves are then generated using the estimated Rayleigh mixture proportions and powers and a non-fluctuating target model. The expected loss in detection performance due to the heavier tails of the non-Rayleigh reverberation was clearly observed.

Keywords

non-Rayleigh – reverberation – statistics

Issuing Organization

North Atlantic Treaty Organization
SACLANT Undersea Research Centre
Viale San Bartolomeo 400, 19138 La Spezia, Italy

[From N. America: SACLANTCEN CMR-426 (New York) APO AE 09613]

Tel: +39 (0)187 540 111
Fax:+39 (0)187 524 600

E-mail: library@saclantc.nato.int

NATO UNCLASSIFIED

Initial Distribution for SR 266

Ministries of Defence

DND Canada	10
CHOD Denmark	8
DGA France	8
MOD Germany	15
HNDGS Greece	12
MARISTAT Italy	10
MOD (Navy) Netherlands	12
NDRE Norway	10
MOD Portugal	5
MDN Spain	2
TDKK and DNHO Turkey	5
MOD UK	20
ONR USA	42

NATO Commands and Agencies

NAMILCOM	2
SACLANT	3
CINCEASTLANT/ COMNAVNORTHWEST	1
CINCIBERLANT	1
CINCWESTLANT	1
COMASWSTRIKFOR	1
COMMAIREASTLANT	1
COMSTRIKFLTANT	1
COMSUBACLANT	1
SACLANTREPEUR	1
SACEUR	2
CINCNORTHWEST	1
CINCSOUTH	1
COMEDCENT	1
COMMARAIRMED	1
COMNAVSOUTH	1
COMSTRIKFORSOUTH	1
COMSUBMED	1
NC3A	1
PAT	1

Scientific Committee of National Representatives

SCNR Belgium	1
SCNR Canada	1
SCNR Denmark	1
SCNR Germany	1
SCNR Greece	1
SCNR Italy	1
SCNR Netherlands	2
SCNR Norway	1
SCNR Portugal	1
SCNR Spain	1
SCNR Turkey	1
SCNR UK	1
SCNR USA	2
French Delegate	1
SECGEN Rep. SCNR	1
NAMILCOM Rep. SCNR	1

National Liaison Officers

NLO Canada	1
NLO Denmark	1
NLO Germany	1
NLO Italy	1
NLO Netherlands	1
NLO UK	1
NLO USA	1

Sub-total	208
SACLANTCEN	30
Total	238